These studies suggest that new therapeutic or vaccine regimens against tuberculosis might be successfully developed by targeting strategies that induce autophagy (Jagannath *et al.*, 2009; Yuk *et al.*, 2009; Jo, 2010).

Coronin-1a (Coro1a) is a member of the coronin family associated with F-actin (de Hostos, 1999) and localizes to mycobacterial phagosomes (Ferrari *et al.*, 1999). Gene silencing of Coro1a was found to prevent *M. tuberculosis* survival in macrophages (Jayachandran *et al.*, 2007; 2008; Kumar *et al.*, 2010). These results suggest that *M. tuberculosis* perverts Coro1a function to allow the survival of this bacterium in macrophages (Pieters, 2008). Currently, the survival mechanisms involved in this process are not fully understood. In this study, we found that the depletion of Coro1a promoted autophagosome formation around *M. tuberculosis*-containing phagosomes in macrophages. The molecular mechanisms of Coro1a-mediated *M. tuberculosis* survival are also discussed.

Results

Depletion of Coro1a in macrophages by siRNA prevents M. tuberculosis *survival*

To deplete Coro1a expression in Raw264.7 macrophages, we employed Coro1a-specific small interfering ribonucleic acids (siRNA) and verified the knock-down (KD) efficiency of Coro1a by immunoblot analysis. We designed two sets of the Coro1a-specific siRNA sequences, one of which is based on the report by Jayachandran *et al.* (2007). More than 90% KD efficiency for the Coro1a protein was obtained by transfection with siRNA duplexes (Fig. 1A). We then examined the survival of *M. tuberculosis* in Raw264.7 macrophages transfected with Coro1a-specific siRNA and confirmed the inhibition of *M. tuberculosis* survival in Coro1a KD macrophages (Fig. 1B) (Jayachandran *et al.*, 2007; 2008; Kumar *et al.*, 2010).

Previous studies demonstrated that lysosomes fused with mycobacterial phagosomes in Coro1a-depleted macrophages (Jayachandran *et al.*, 2007; 2008), suggesting that the inhibition of phagolysosomal biogenesis is associated with the Coro1a-dependent survival of *M. tuberculosis*.

In this study, we examined the acidification of mycobacterial phagosomes and their fusion with lysosomes in Coro1a KD macrophages (Fig. 2). Coro1a KD macrophages were infected with DsRed-expressing *M. tuberculosis* for 24 h and examined the acidification of mycobacterial phagosomes and their fusion with lysosomes by staining with LysoTracker and anti-LAMP1 antibody respectively. The proportion of LysoTracker-positive (Fig. 2A and B) and LAMP1-positive (Fig. 2C and D) mycobacterial phagosomes increased in Coro1a KD

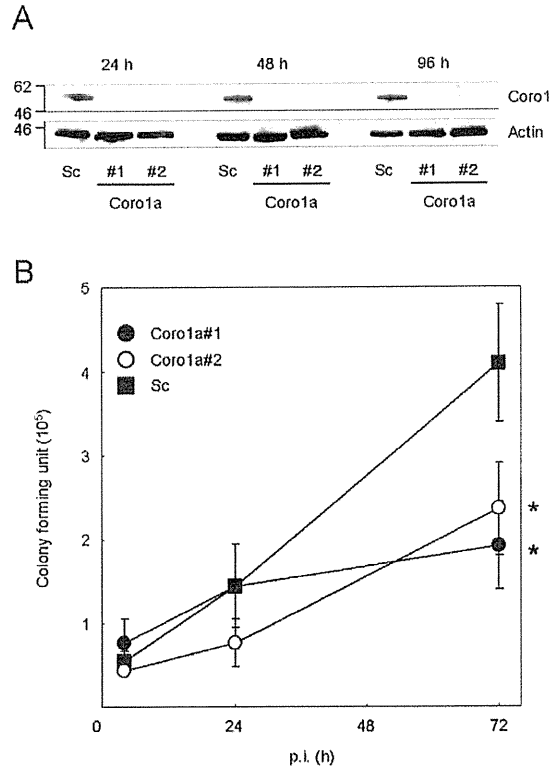

Fig. 1. Survival of *M. tuberculosis* in Coro1a KD macrophages.
A. Immunoblot analysis of Coro1a KD macrophages. Raw264.7 macrophages were transfected with Coro1a-specific or scrambled (Sc) siRNA for 24, 48 and 96 h. Whole-cell lysates from transfected macrophages were subjected to SDS-PAGE, followed by immunoblot analysis using the indicated antibodies.
B. Proliferation of *M. tuberculosis* in Coro1a KD macrophages. Macrophages were transfected with Coro1a or scrambled siRNA for 24 h and then infected with *M. tuberculosis*. The number of viable mycobacteria was determined using a colony-forming unit (cfu) assay at 4, 24 and 72 h post infection (p.i.). The data represent the means and the standard error of the means (SEM) of three independent experiments. The numbers of cfu at 72 h p.i. in macrophages transfected with Coro1a and scrambled siRNA were compared. $^*P < 0.05$ (unpaired Student's *t*-test).

macrophages. These results suggest that the maturation of mycobacterial phagosomes is promoted in Coro1a KD macrophages.

Autophagy is involved in the inhibition of M. tuberculosis *survival in Coro1a KD macrophages*

We next focused on the effect that Coro1a depletion had on the induction of autophagy in macrophages infected with *M. tuberculosis*, because autophagy is known to be associated with *M. tuberculosis* eradication (Deretic *et al.*, 2006; 2009; Jo, 2010; Lerena *et al.*, 2010). To investigate the involvement of autophagy, Coro1a KD macrophages were treated with 3-methyladenine (3-MA), an autophagy

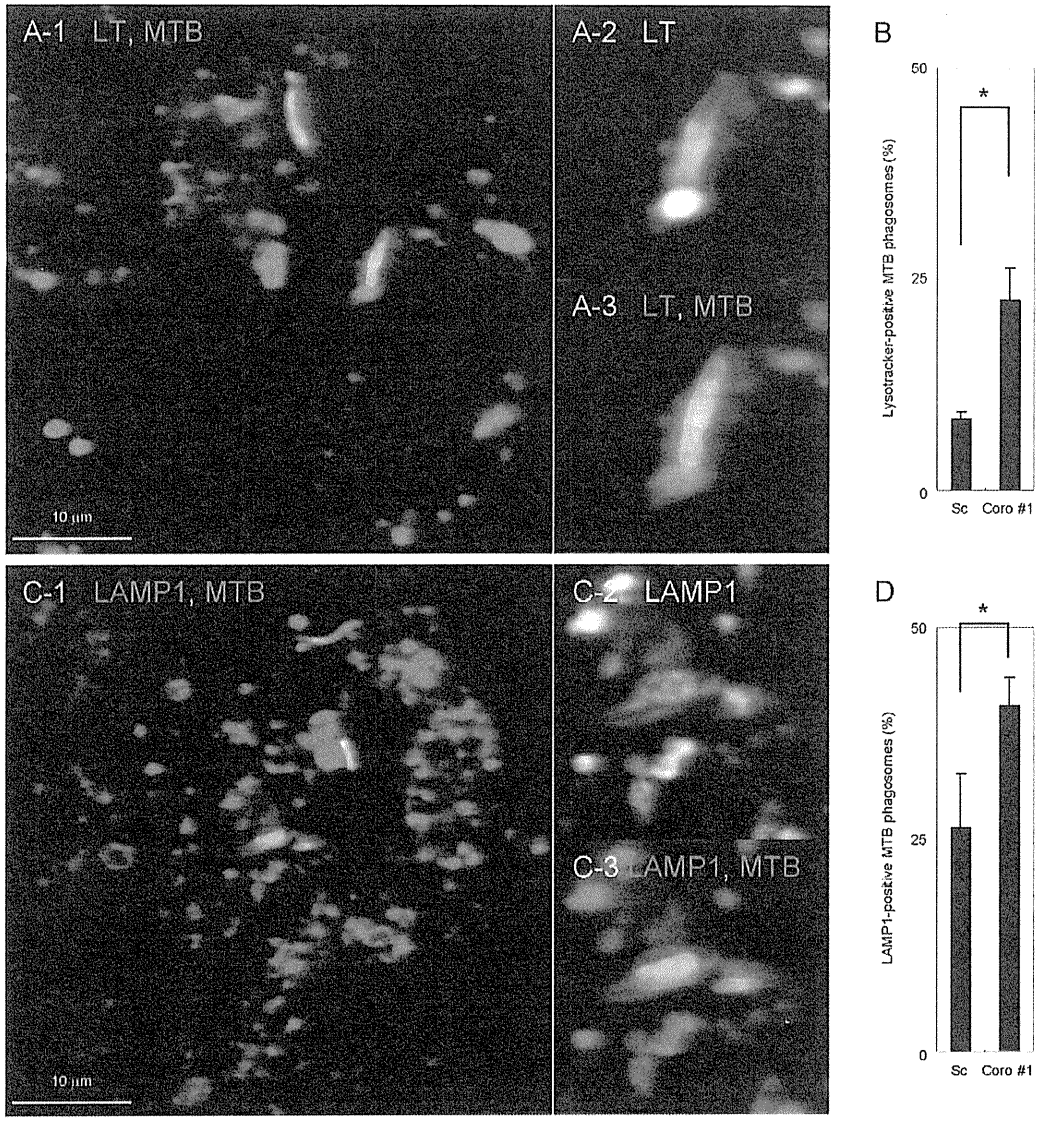

Fig. 2. Maturation of *M. tuberculosis*-containing phagosomes in Coro1a KD macrophages.
A. Acidification of mycobacterial phagosomes in Coro1a KD macrophages. Macrophages transfected with Coro1a-specific siRNA were infected with DsRed-expressing *M. tuberculosis* for 24 h and stained with LysoTracker. Infected macrophages were fixed and observed by laser scanning confocal microscopy (LSCM). Enlarged images of A-1 are represented in A-2 and A-3.
B. The proportion of *M. tuberculosis*-containing phagosomes labelled with LysoTracker in Coro1a KD macrophages. The numbers of LysoTracker-positive *M. tuberculosis*-containing phagosomes in macrophages transfected with Coro1a-specific or scrambled siRNA were counted.
C. LAMP1 localization to mycobacterial phagosomes in Coro1a KD macrophages. Macrophages transfected with Coro1a-specific siRNA were infected with DsRed-expressing *M. tuberculosis* for 24 h. Infected macrophages were stained with anti-LAMP1 antibody and observed by LSCM. Enlarged images of C-1 are represented in C-2 and C-2.
D. The proportion of *M. tuberculosis*-containing phagosomes labelled with anti-LAMP1 antibody in Coro1a KD macrophages. The numbers of LAMP1-positive *M. tuberculosis*-containing phagosomes in macrophages transfected with Coro1a-specific or scrambled siRNA were counted. Data represent the means and the standard deviations (SD) of three independent experiments in which more than 200 phagosomes were counted for each condition. $^*P < 0.05$ (unpaired Student's *t*-test); Sc, scrambled; Coro, Coro1a; MTB, *M. tuberculosis*; LT, LysoTracker.

inhibitor (Seglen and Gordon, 1982), and then infected with *M. tuberculosis*. The survival of *M. tuberculosis* in Coro1a KD macrophages was partially restored by treatment with 3-MA (Fig. 3A), suggesting that autophagic processes were involved in the inhibition of mycobacterial survival in Coro1a KD macrophages.

To further analyse the inhibitory mechanism of *M. tuberculosis* survival, we infected macrophages co-transfected with siRNAs for Coro1a and autophagy-related genes with *M. tuberculosis*. Atg3, Atg5 and Beclin1 are well-known autophagy-related proteins that drive the autophagy process (Mizushima and Levine, 2010). The targeting efficiencies of Coro1a and autophagy-related genes in Raw264.7 macrophages were confirmed by immunoblot analysis (Fig. 3E). Silencing of these autophagy-related proteins restored this inhibitory effect on *M. tuberculosis* survival in Coro1a KD macrophages (Fig. 3B–D). These results suggest that the induction of autophagy is involved in the promotion of *M. tuberculosis* eradication in Coro1a KD macrophages.

Autophagosome formation around M. tuberculosis*-containing phagosomes in Coro1a KD macrophages*

To confirm autophagosome formation in Coro1a KD macrophages infected with *M. tuberculosis*, we examined the localization of LC3, an autophagosome marker (Kabeya *et al.*, 2000), by fluorescence microscopy. Coro1a KD or control Raw264.7 macrophages were infected with DsRed-expressing *M. tuberculosis* and stained with anti-LC3 antibody. Only a small population of *M. tuberculosis*-containing phagosomes was LC3-positive in the control macrophages at 6 h post infection (p.i.) (Fig. 4A), supporting previous findings (Gutierrez *et al.*, 2004). LC3 recruitment to the mycobacterial phagosomes was further observed in Coro1a KD macrophages (Fig. 4B). Quantitative analysis revealed that the proportion of LC3-positive mycobacterial phagosomes was $>30\%$ and $<10\%$ in Coro1a KD and control macrophages respectively (Fig. 4E). Similar experiments employing LC3 fused with enhanced green fluorescence protein (EGFP-LC3) were also conducted. Raw264.7 macrophage stably expressing EGFP-LC3 were infected with DsRed-expressing *M. tuberculosis* for 2, 6 or 24 h. LC3 again localized to a small population of mycobacterial phagosome in control macrophages (Fig. 4C), while the number of LC3-positive mycobacterial phagosomes increased in Coro1a KD macrophages at 6 h p.i. (Fig. 4D). Quantitative analysis revealed that the proportion of LC3-positive mycobacterial phagosomes in Coro1a KD macrophages was greater than 30% and 20% at 6 h and 24 h p.i., respectively, while such an increase was not observed in control macrophages (Fig. 4F).

The ultrastructure of *M. tuberculosis*-containing phagosomes in Coro1a KD macrophages was also observed by thin-section electron microscopy. In control macrophages, bacilli resided in single-membrane phagosomes (Fig. 5A). In contrast, bacilli were surrounded by multiple membrane structures that were characteristic of autophagic vacuoles (Eskelinen, 2005) in Coro1a KD macrophages (Fig. 5B). We also found mycobacterial phagosomes with internal membranes in Coro1a KD macrophages (Fig. 5C) as previously reported (Gutierrez *et al.*, 2004). Quantitative analysis revealed that the proportion of bacilli associated with autophagic membrane structures reached more than 30% in Coro1a KD macrophages while that in control macrophages was less than 10% at 6 h p.i. (Fig. 5D). Collectively, these fluorescence and electron microscopy results suggest that autophagosome formation is induced around *M. tuberculosis*-containing phagosomes in Coro1a KD macrophages.

Validation of LC3 recruitment to M. tuberculosis*-containing phagosomes in Coro1a KD macrophages*

The recruitment of LC3 to *M. tuberculosis*-containing phagosomes was subsequently investigated in Coro1a KD macrophages treated with 3-MA (Fig. 6A) or simultaneously transfected with siRNA duplexes for autophagy-related genes (Fig. 6B). Both treatments abrogated the induction of LC3 recruitment to mycobacterial phagosomes in Coro1a KD macrophages.

Upon autophagy induction, LC3 is processed from a cytosolic form (LC3-I) to a membrane bound form (LC3-II) (Kabeya *et al.*, 2000). We first attempted to confirm the autophagy induction by immunoblot analysis using whole-cell lysates, but no significant increase in LC3 processing was observed in Coro1a KD and control macrophages infected with *M. tuberculosis* (Fig. 7A and D). We also found that no significant changes of LC3 processing in control or Coro1a KD macrophages infected with *M. tuberculosis* at the different infection rates (Fig. S1). The treatment with NH_4Cl or bafilomycin A1 achieved the similar accumulation of LC3-II in both control and Coro1a KD macrophages infected with *M. tuberculosis* (Fig. 7B and E), suggesting the normal autophagic flux in these macrophages. We next examined the recruitment of LC3 using isolated *M. tuberculosis*-containing phagosomes in Coro1a KD macrophages by immunoblot analysis (Fig. 7C). Enrichment of LC3-II was observed in the phagosomal fraction from Coro1a KD macrophages when compared with that from the control macrophages. Densitometric analysis revealed that the amount of LC3-II in the phagosomal fraction from Coro1a KD macrophages increased to approximately 2.7 times that observed for the control macrophages (Fig. 7F). This biochemical analysis

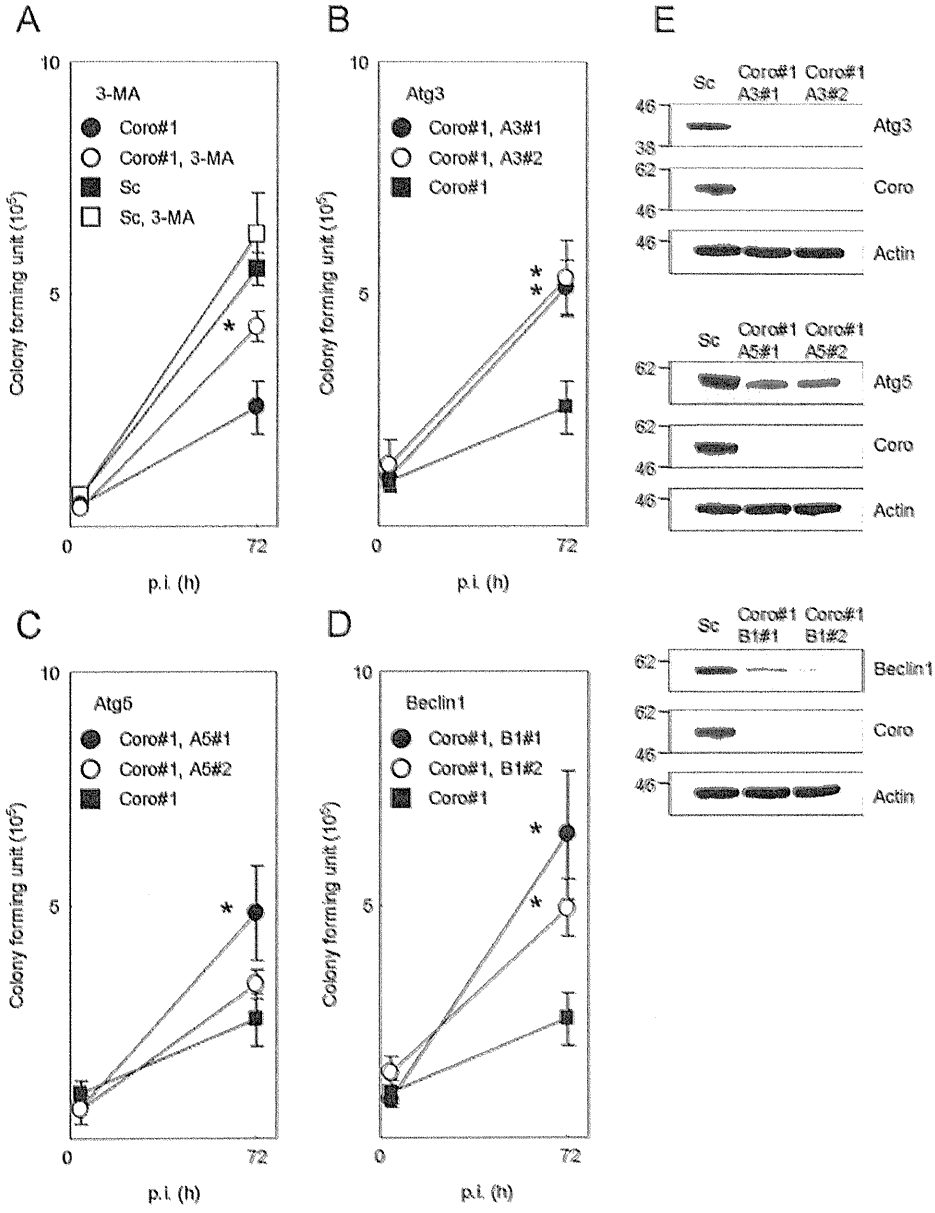

Fig. 3. Treatment with 3-MA or siRNA for autophagy-related genes suppressed the inhibition of *M. tuberculosis* proliferation in Coro1a KD macrophages.

A. Proliferation of *M. tuberculosis* in Coro1a KD macrophages treated with 3-MA. Macrophages transfected with Coro1a-specific or scrambled siRNA were treated with or without 3-MA (10 mM) for 1 h and then infected with *M. tuberculosis*. Viable mycobacteria number was determined by cfu assay at 4 h and 72 h p.i. The data represent the means and SEM of three independent experiments. The numbers of cfu at 72 p.i. in Coro1a KD macrophages treated with or without 3-MA were compared. $*P < 0.05$ (unpaired Student's *t*-test).

B–D. Proliferation of *M. tuberculosis* in macrophages transfected with siRNA for Coro1a and autophagy-related genes. Macrophages were transfected with siRNAs for Coro1a and Atg3 (B), Coro1a and Atg5 (C) or Coro1a and Beclin1 (D). Transfected macrophages were then infected with *M. tuberculosis*. Colony-forming unit assay was performed at 4 h and 72 h p.i. The data represent the means and SEM of three independent experiments. The numbers of cfu at 72 h p.i. in Coro1a KD macrophages transfected with or without siRNA for autophagy-related genes were compared. $*P < 0.05$ (unpaired Student's *t*-test).

E. Immunoblot analysis on the silencing effects of Coro1a and autophagy-related genes. Macrophages were transfected with siRNA for Coro1a and the indicated autophagy-related genes for 48 h. Whole-cell lysates were subjected to SDS-PAGE, followed by immunoblot analysis using the indicated antibodies.

Sc, scrambled; Coro, Coro1a; A3, Atg3; A5, Atg5; B1, Beclin1.

further supports that the recruitment of LC3 to *M. tuberculosis*-containing phagosomes is facilitated by Coro1a depletion in macrophages.

Localization of p62, ubiquitin and LAMP1 to LC3-positive mycobacterial phagosomes in Coro1a KD macrophages

To characterize the LC3-positive mycobacterial phagosomes in Coro1a KD macrophages, we examined the localization of p62/SQSTM1 (p62), ubiquitin and LAMP1 to LC3-positive mycobacterial phagosomes (Fig. 8). Bacteria in cytosols are targeted by the ubiquitin system (Perrin *et al.*, 2004) and the autophagic degradation (Dupont *et al.*, 2009). p62 is involved in targeting intracellular bacteria to the autophagy pathway (Dupont *et al.*, 2009; Zheng *et al.*, 2009) and indispensable for autophagic elimination of mycobacteria in macrophages (Ponpuak *et al.*, 2011). We found that p62 and ubiquitin localized to LC3-positive mycobacterial phagosomes in Coro1a KD macrophages (Fig. 8A and C). The proportion of LC3-positive mycobacterial phagosomes colocalized with p62 and/or ubiquitin increased up to 24 h p.i. (Fig. 8B and D). In addition, the proportion of LC3-positive mycobacterial phagosomes colocalized with LAMP1 also increased up to 24 h p.i. (Fig. 8E and F). These results indicate that p62, ubiquitin and/or LAMP1 are recruited to LC3-positive mycobacterial phagosomes in Coro1a KD macrophages during infection.

Phosphorylation of p38 MAPK is induced by M. tuberculosis *infection in Coro1a KD macrophages*

As mitogen-activated protein kinase (MAPK) signalling pathways are involved in autophagy induction (Esclatine *et al.*, 2009), we next examined which MAPK signalling pathways were affected by *M. tuberculosis* infection in Coro1a KD macrophages (Fig. 9). Macrophages transfected with Coro1a-specific or scrambled siRNA were infected with *M. tuberculosis*, and phosphorylation of ERK1/2, p38 and JNK was investigated by immunoblot analysis. No significant difference in ERK1/2 activation kinetics was detected between control and Coro1a KD macrophages after *M. tuberculosis* infection. JNK activation was not detected in both control and Coro1a KD macrophages (data not shown). In contrast, a significant increase in p38 phosphorylation was observed in Coro1a KD macrophages, while no induction was detected in control macrophages (Fig. 9A).

The recruitment of LC3 to *M. tuberculosis*-containing phagosomes in Coro1a KD macrophages treated with various inhibitors for MAPK signalling pathways was also investigated by imaging analysis. Inhibition of p38 signalling, but not MEK1 or JNK signalling, reduced the proportion of LC3-positive mycobacterial phagosomes in Coro1a KD macrophages (Fig. 9B), further supporting that the p38 MAPK pathway is a target of Coro1a in the inhibition of autophagosome formation around *M. tuberculosis*-containing phagosomes.

Induction of LC3 recruitment to M. tuberculosis*-containing phagosomes in Coro1a KD alveolar macrophages and bone marrow-derived macrophages*

Mycobacterium tuberculosis is inhaled via aerosols into the lung, where alveolar macrophages (AM) are the first line of defence (Russell, 2001; 2007). We investigated whether autophagosome formation around *M. tuberculosis*-containing phagosomes is also induced in AM by Coro1a depletion. MH-S is an AM cell line, in which *M. tuberculosis* can survive and proliferate (Mbawuike and Herscowitz, 1989; Sirakova *et al.*, 2003). MH-S macrophages were transfected with Coro1a siRNA (Fig. 10A) and infected with *M. tuberculosis*. When AM were transfected with scrambled siRNA, LC3 did not localize to mycobacterial phagosomes (data not shown). In contrast, the recruitment of LC3 to mycobacterial phagosomes increased in Coro1a KD AM (Fig. 10B). Quantitative analysis revealed that the proportions of LC3-positive mycobacterial phagosomes were $> 25\%$ and $< 5\%$ in Coro1a KD and control AM respectively (Fig. 10C). We also examined the localization of LC3 to mycobacterial phagosomes in bone marrow-derived macrophages (BMDM) transfected with Coro1a-specific or scrambled siRNA (Fig. 10A). The depletion of Coro1a also induced the recruitment of LC3 to *M. tuberculosis*-containing phagosomes in BMDM (Fig. 10D). Quantitative analysis revealed that approximately 10% and 2% of mycobacterial phagosomes were LC3 positive in Coro1a KD and control BMDM respectively (Fig. 10E). Treatment with 3-MA reduced the proportion of LC3-positive mycobacterial phagosomes in Coro1a KD macrophages (Fig. 10F). These results suggest that autophagosome formation around *M. tuberculosis*-containing phagosomes is also induced in AM and BMDM as a consequence of Coro1a depletion.

Discussion

Coro1a was initially reported being retained on phagosomes containing live mycobacteria, while being rapidly released from phagosomes containing inactive mycobacteria (Ferrari *et al.*, 1999). Genetic depletion or RNA interference-mediated gene silencing of Coro1a was later reported inhibiting the survival of mycobacteria within macrophages (Jayachandran *et al.*, 2007; 2008; Kumar *et al.*, 2010). In this study, we confirmed that the survival

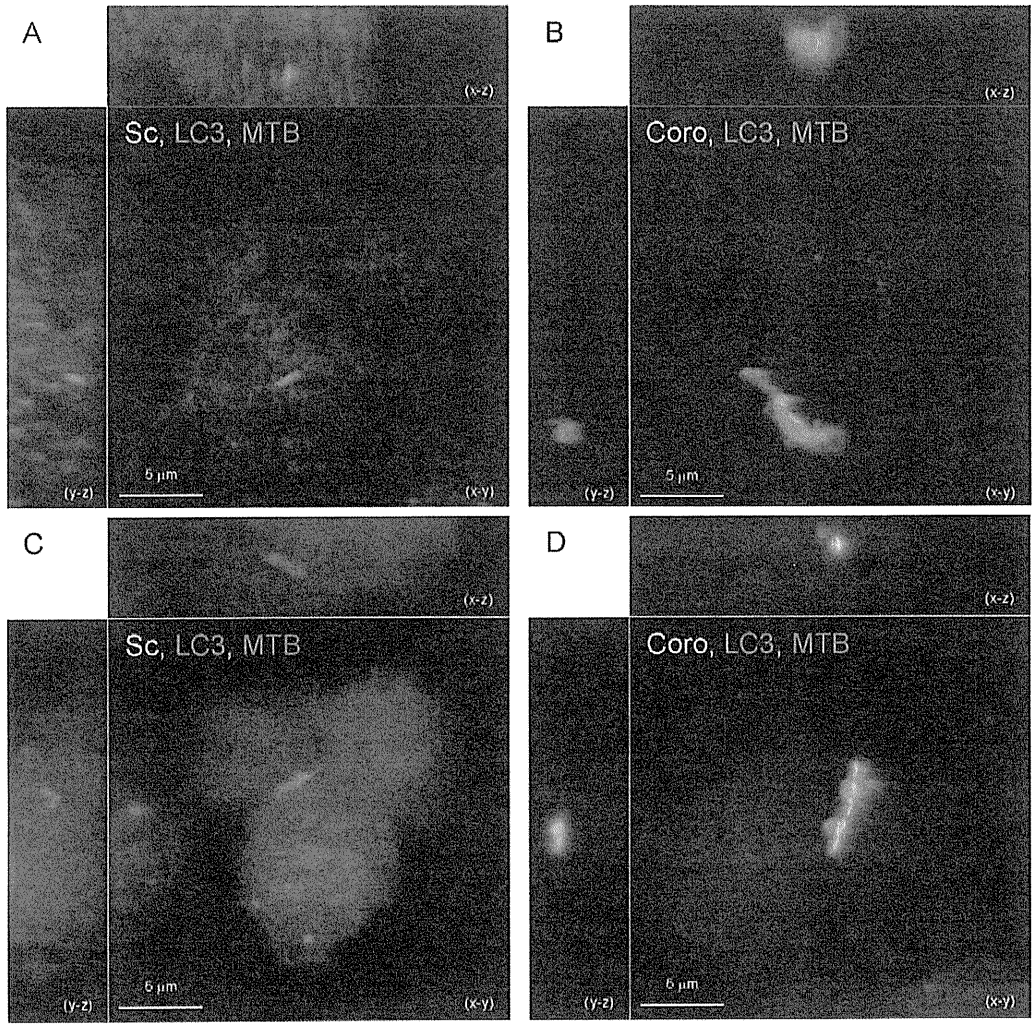
A
Sc, LC3, MTB
(x-z)
(y-z)
5 μm
(x-y)
B
Coro, LC3, MTB
(x-z)
(y-z)
5 μm
(x-y)
C
Sc, LC3, MTB
(x-z)
(y-z)
5 μm
(x-y)
D
Coro, LC3, MTB
(x-z)
(y-z)
5 μm
(x-y)

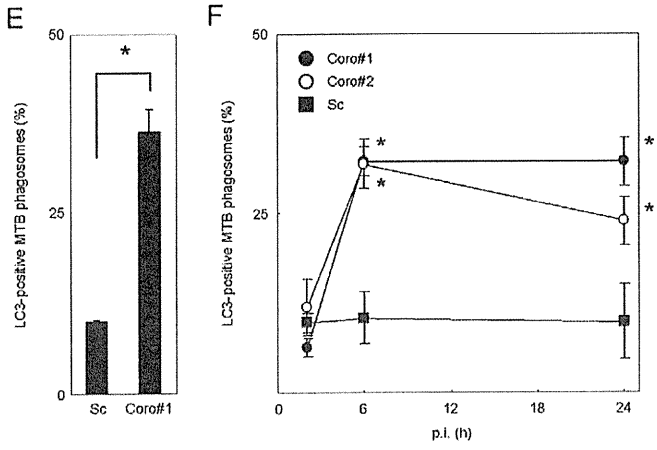
E
LC3-positive MTB phagosomes (%)
50
25
0
*
Sc
Coro#1
F
LC3-positive MTB phagosomes (%)
50
25
0
Coro#1
Coro#2
Sc
*
*
*
*
0
6
12
18
24
p.i. (h)

Fig. 4. LC3 recruitment to mycobacterial phagosomes in Coro1a KD macrophages.
A and B. LC3 recruitment to *M. tuberculosis*-containing phagosomes in Coro1a KD macrophages by immunofluorescence microscopy. Macrophages transfected with scrambled (A) or Coro1a-specific (B) siRNA were infected with DsRed-expressing *M. tuberculosis* for 6 h. Infected macrophages were fixed and stained with anti-LC3 antibody, and then observed with LSCM. Projections of focal planes with y–z and x–z side views are represented.
C and D. Recruitment of LC3 fused with EGFP (EGFP-LC3) to *M. tuberculosis*-containing phagosomes in Coro1a KD macrophages. Macrophages stably expressing EGFP-LC3 were transfected with scrambled (C) or Coro1a-specific (D) siRNA and infected with DsRed-expressing *M. tuberculosis* for 6 h. Infected macrophages were fixed and observed by LSCM. Projections of focal planes with y–z and x–z side views are represented.
E. The proportion of *M. tuberculosis*-containing phagosomes labelled with anti-LC3 antibody in Coro1a KD macrophages. Macrophages transfected with Coro1a-specific or scrambled siRNA were infected with DsRed-expressing *M. tuberculosis* for 6 h. Cells were then stained with anti-LC3 antibody and observed with LSCM. The number of LC3-positive *M. tuberculosis*-containing phagosomes was counted.
F. The proportion of *M. tuberculosis*-containing phagosomes labelled with EGFP-LC3. Macrophages stably expressing EGFP-LC3 were transfected with Coro1a or scrambled siRNA and infected with DsRed-expressing *M. tuberculosis* for 2, 6 and 24 h. Cells were fixed and observed with LSCM. The numbers of LC3-positive mycobacterial phagosomes were counted.
Data represent the mean and SD of three independent experiments in which more than 200 phagosomes were counted for each condition. $^*P < 0.05$ (unpaired Student's *t*-test). Sc, scrambled; Coro, Coro1a; MTB, *M. tuberculosis*.

of *M. tuberculosis* was inhibited in Coro1a KD macrophages (Fig. 1). However, the infection rate of *M. tuberculosis* with Coro1a KD macrophages possibly affects its proliferation within infected macrophages, because a previous study demonstrated that the expression of a dominant-negative form of Coro1a or transfection of Coro1a siRNA decreased the activity of phagocytosis (Yan *et al.*, 2005). To address this possibility, we examined the phagocytosis rate of latex beads and the infection rate of *M. tuberculosis* in Coro1a KD macrophages but found no differences in these events between Coro1a KD and control macrophages (Fig. S2). Previous studies demonstrated that the phagolysosome biogenesis of mycobacterial phagosomes occurred by the depletion of Coro1a in macrophages (Jayachandran *et al.*, 2007; 2008). We also found that the acidification and the fusion of lysosomes with mycobacterial phagosomes were promoted in Coro1a KD macrophages (Fig. 2). However, there has been no direct evidence that the inhibition of mycobacterial proliferation in Coro1a KD macrophages is caused by the promotion of phagolysosome biogenesis.

We hypothesized that autophagy is induced in Coro1a KD macrophages and inhibits *M. tuberculosis* survival. This is because the inhibition of autophagy by 3-MA or gene silencing of autophagy-related genes restores the mycobacterial survival in Coro1a KD macrophages (Fig. 3). To verify this hypothesis, we examined the localization of LC3 and found that LC3 was recruited to *M. tuberculosis*-containing phagosomes in Coro1a KD macrophages (Fig. 4). Thin-section electron microscopy revealed that *M. tuberculosis*-containing phagosomes were surrounded by characteristic autophagic membrane structures in Coro1a KD macrophages (Fig. 5). Treatment with 3-MA or silencing of autophagy-related genes inhibited the recruitment of LC3 to *M. tuberculosis*-containing phagosomes in Coro1a KD macrophages (Fig. 6). It is reported that the delivery of anti-bactericidal protein and/or peptides to mycobacterial phagosomes depended on the induction of autophagy (Alonso *et al.*, 2007; Yuk *et al.*, 2009; Ponpuak *et al.*, 2011). We also showed that the proportion of LC3-positive mycobacterial phagosomes colocalized with p62, ubiquitin and LAMP1 increased in Coro1a KD macrophages up to 24 h p.i., suggesting the involvement of the ubiquitin system and autophagic degradation. Combined, these results suggest that the inhibition of mycobacterial proliferation in Coro1a KD macrophages is caused by the autophagosome formation around mycobacterial phagosomes and subsequent bactericidal effector mechanisms.

In the present study, we sought key events for the induction of autophagosome formation around *M. tuberculosis*-containing phagosomes induced by Coro1a depletion. Immunoblot analysis using whole-cell lysates revealed that the *M. tuberculosis* infection itself did not stimulate whole-cell LC3 processing in Coro1a KD macrophages (Fig. 7 and Fig. S1), because there was no difference in autophagic flux between control and Coro1a KD macrophages infected with *M. tuberculosis* (Fig. 7). Immunofluorescence microscopy also demonstrated that *M. tuberculosis* infection did not induce the formation of punctuated LC3 structures in Coro1a KD macrophages (Fig. 4). In addition, *M. tuberculosis* is thought to prevent the induction of autophagy by inhibiting PI3-kinase activation via the bacterial cell wall component, lipoarabinomannan or a secreted phosphatase (Vergne *et al.*, 2003; 2004; Deretic *et al.*, 2004; 2006). Present results suggest that *M. tuberculosis* infection itself cannot induce autophagy within the cytosol of Coro1a KD macrophages unlike nutrient starvation or pharmacological autophagy inducers.

It is reported that Coro1a regulated the activity of calcineurin and that the calcineurin inhibitors stimulated the fusion of lysosomes with mycobacterial phagosomes (Jayachandran *et al.*, 2007). In *Caenorhabditis elegans*, a loss-of-function or null mutation of calcineurin induces the autophagosome formation (Dwivedi *et al.*, 2009). These results imply that autophagosome formation around mycobacterial phagosomes is caused by the inhibition of

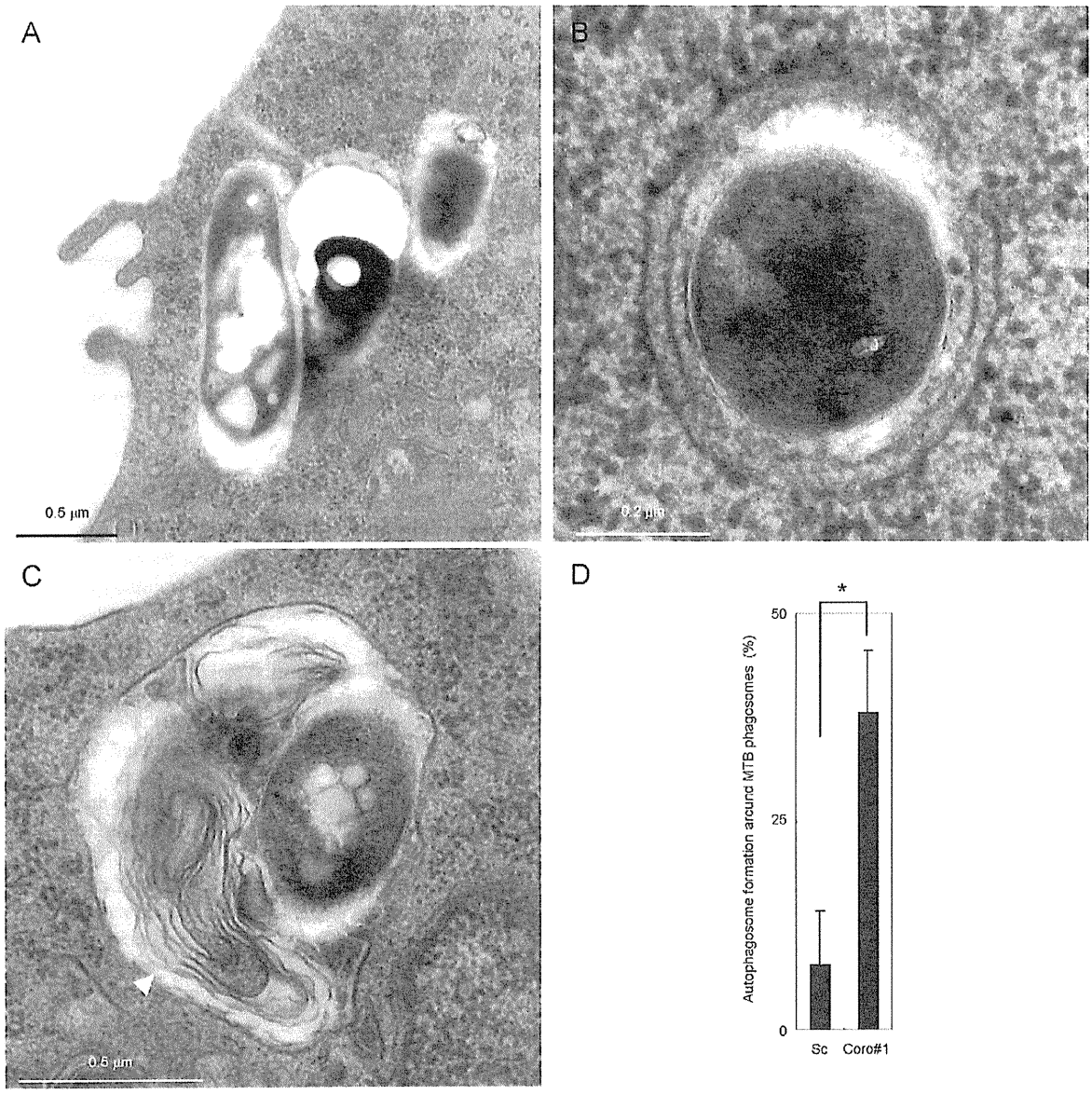

Fig. 5. Thin-section electron micrographs of Coro1a KD macrophages infected with *M. tuberculosis*.
A–C. Macrophages were transfected with scrambled (A) or Coro1a-specific (B, C) siRNA and then infected with *M. tuberculosis* for 6 h. Infected macrophages were fixed and observed with thin-section electron microscopy. An arrowhead indicates the internal membrane in the mycobacterial phagosome.
D. The proportion of *M. tuberculosis*-containing phagosomes associated with multiple membrane structures in Coro1a KD macrophages. Macrophages transfected with Coro1a-specific or scrambled siRNA were infected with *M. tuberculosis* for 6 h. Cells were fixed and observed with thin-section electron microscopy. The number of *M. tuberculosis*-containing phagosomes with multiple membrane structures was counted. Data represent the mean and SD of three independent experiments in which more than 50 phagosomes were counted for each condition.
*$P < 0.05$ (unpaired Student's *t*-test). Sc, scrambled; Coro, Coro1a; MTB, *M. tuberculosis*.

calcineurin activity in Coro1a KD macrophages. We examined whether the inhibition of calcineurin activity induced the autophagosome formation around *M. tuberculosis*-containing phagosomes but found no induction of LC3 recruitment to the phagosomes in macrophages treated with FK506 or cyclosporine A (Fig. S3). Bcl-2 is a member of the anti-apoptotic proteins and interacts with Beclin1 to inhibit the induction of autophagy (Pattingre *et al.*, 2005). The expression of Bcl-2 is reduced in naïve T cells from Coro1a-deficient mice (Mueller *et al.*, 2011). We therefore

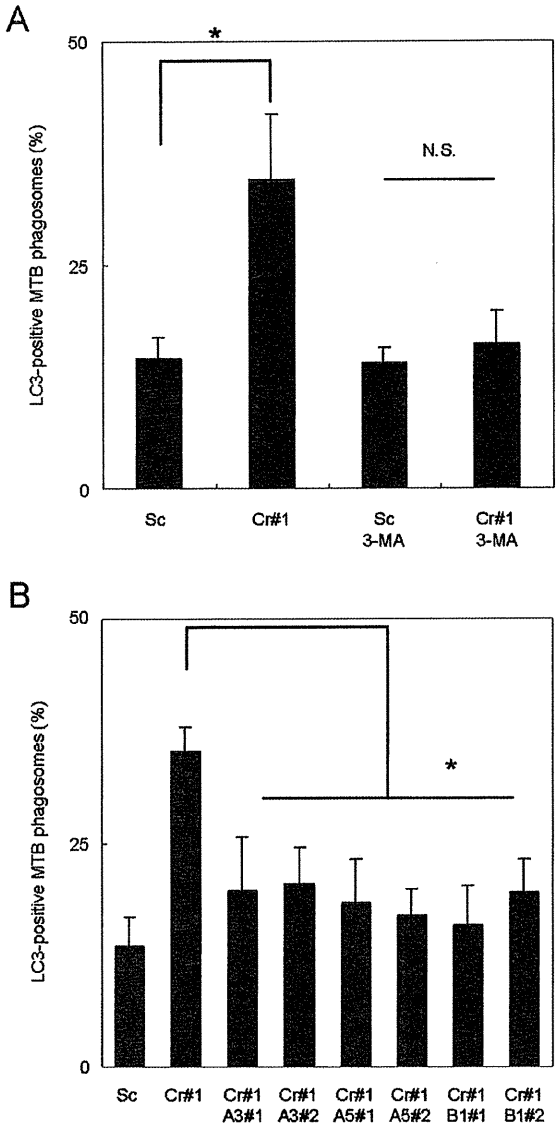

Fig. 6. LC3 recruitment to *M. tuberculosis*-containing phagosomes in Coro1a KD macrophages treated with 3-MA or siRNA for autophagy-related genes. The proportion of LC3-positive mycobacterial phagosomes in Coro1a KD macrophages treated with 3-MA at 10 mM (A) or transfected with siRNA for autophagy-related genes (B). Data represent the mean and SD of three independent experiments in which more than 200 phagosomes were counted for each condition. $^*P < 0.05$; N.S., not significant (unpaired Student's *t*-test). Sc, scrambled; Cr, Coro1a; A3, Atg3; A5, Atg5; B1, Beclin1.

addressed whether autophagosome formation around *M. tuberculosis*-containing phagosomes by Coro1a depletion is accompanied by the downregulation of Bcl-2 and found no significant change in Bcl-2 expression between control and Coro1a KD macrophages (Fig. S4). It is also reported that the transcription of Coro1a is downregulated by the combination of vitamin D3 and retinoic acid in human macrophages (Anand and Kaul, 2003). Vitamin D3 is also reported inducing autophagy in monocyte, resulting in the elimination of infected mycobacteria (Yuk *et al.*, 2009). These reports imply that vitamin D3 decreases the expression of Coro1a in mycobacteria-infected macrophages, leading the autophagosome formation and elimination of infected mycobacteria.

A recent report demonstrated that LC3 is recruited to *Mycobacterium marinum*-containing phagosomes depending on the function of ESX-1 (Lerena and Colombo, 2011). ESAT-6 homologue of *M. marinum* has a pore formation activity in phagosomal membranes and assists the bacilli to escape from phagosomes to cytosol and move by actin-based motility (Stamm *et al.*, 2003; Gao *et al.*, 2004; Smith *et al.*, 2008). *M. tuberculosis* is also reported to translocate from its containing phagosomes to cytosols in infected monocytes depending on ESX-1 secretion system (van der Wel *et al.*, 2007), suggesting that the secreted proteins including ESAT-6 by ESX-1 system damage the phagosomal membranes. Since Coro1a interacts with F-actin to stabilize the structure (Galkin *et al.*, 2008), it is likely that Coro1a localization to mycobacterial phagosomes (Ferrari *et al.*, 1999) supports the phagosomal membranes and that the depletion of Coro1a increases the susceptibility of the phagosomal membranes to ESAT-6 secreted by *M. tuberculosis*. The damage on the membrane of *M. tuberculosis*-containing phagosome could induce the autophagosome formation (Lerena *et al.*, 2010) in Coro1a KD macrophages.

We examined the activation of MAPK signalling pathways involved in autophagosome formation around mycobacterial phagosomes in Coro1a KD macrophages (Fig. 9), as they are involved in autophagy induction (Esclatine *et al.*, 2009). Activation of p38 is indispensable for the induction of autophagy via Toll-like receptor signalling pathways in innate immunity (Xu *et al.*, 2007). JNK signalling pathway was previously reported being involved in the induction of autophagy in macrophages infected with the *eis*-deletion mutant of *M. tuberculosis* (Shin *et al.*, 2010). We assessed the phosphorylation of three MAPKs (ERK-1/2, JNK and p38) and found that only the p38 pathway was specifically activated by *M. tuberculosis* infection in Coro1a KD macrophages (Fig. 9). These results suggest that Coro1a blocks the signal(s) for p38 MAPK activation in response to *M. tuberculosis* infection.

AM are the first defence line of the lung against *M. tuberculosis* infection (Russell, 2001; 2007). We found that the depletion of Coro1a induced autophagosome formation surrounding *M. tuberculosis*-containing phagosomes also in AM and BMDM (Fig. 10). These results suggest that the inhibition of autophagosome formation by

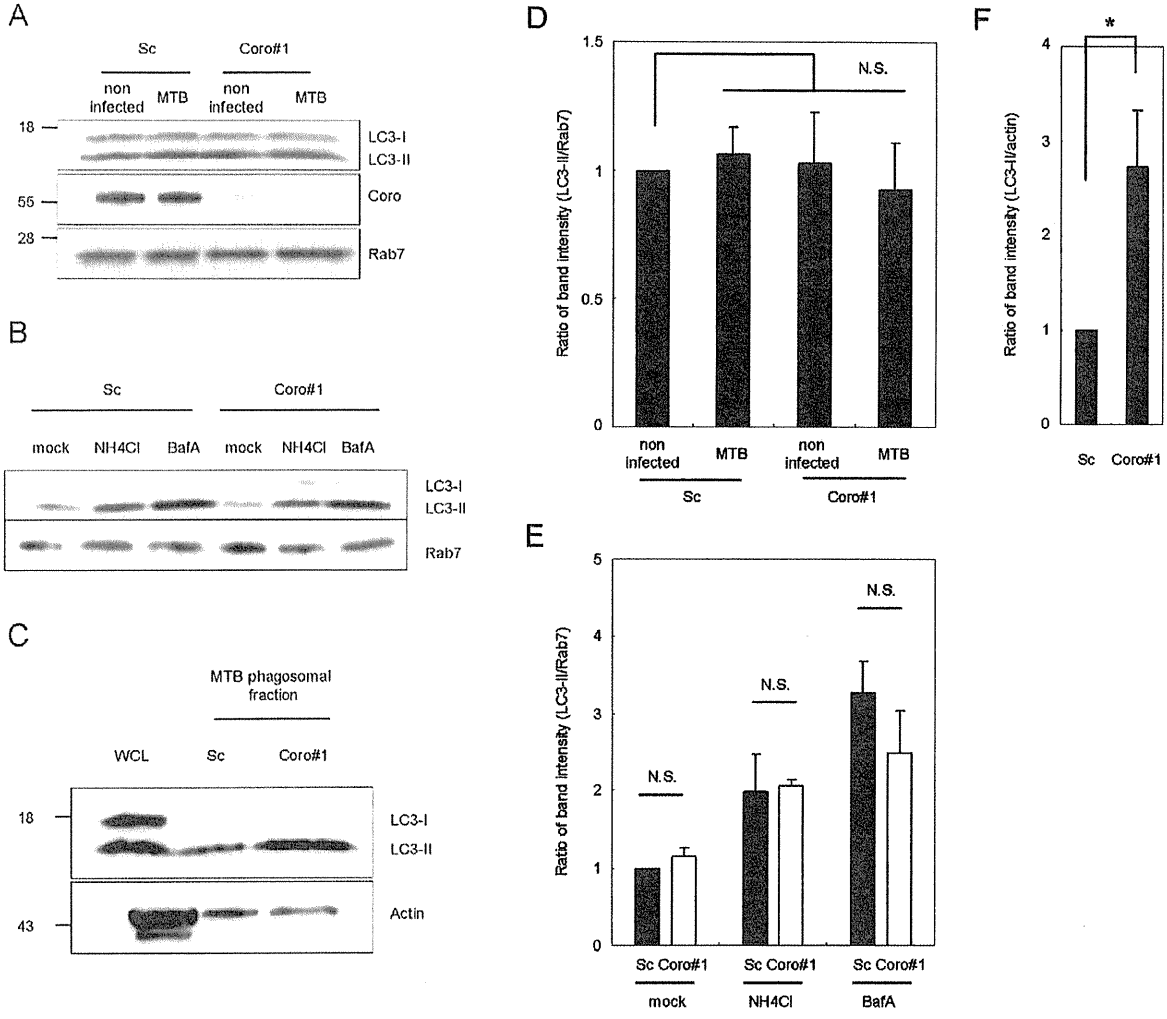

Fig. 7. Immunoblot analysis of LC3 in Coro1a KD macrophages infected with *M. tuberculosis*.
A. Monitoring LC3 processing in Coro1a KD macrophages infected with *M. tuberculosis*. Macrophages transfected with Coro1a-specific or scrambled siRNA were infected with *M. tuberculosis* for 6 h. Whole-cell lysates from non-infected or infected macrophages were subjected to SDS-PAGE, followed by immunoblot analysis using the indicated antibodies.
B. Autophagic flux in Coro1a KD macrophages infected with *M. tuberculosis*. Macrophages transfected with Coro1a-specific or scrambled siRNA were infected with *M. tuberculosis* for 6 h. Infected macrophages were then treated with NH_4Cl (10 mM) or Bafilomycin A1 (10 nM) for 2 h. Whole-cell lysates were subjected to SDS-PAGE, followed by immunoblot analysis using the indicated antibodies.
C. LC3 recruitment to isolated mycobacterial phagosomes. Macrophages transfected with Coro1a or scrambled siRNA were infected with *M. tuberculosis* for 6 h, and phagosomal fractions were isolated as previously described (Beatty *et al.*, 2002; Seto *et al.*, 2011). Whole-cell lysates and phagosomal fractions were subjected to SDS-PAGE, followed by immunoblot analysis using the indicated antibodies.
D–F. Quantification of band intensity for LC3-II. The quantification of band intensity for LC3-II in (A), (B) and (C) was shown in (D), (E) and (F) respectively. The ratio of the band intensity for LC3-II/Rab7 or actin at each condition to that in the macrophage transfected with scrambled siRNA is shown. The data represent the mean and SD of three independent experiments.
*$P < 0.05$; N.S., not significant (paired Student's *t*-test). MTB, *M. tuberculosis*; Sc, scrambled; Coro, Coro1a; NH4Cl, ammonium chloride (NH_4Cl); BafA, Bafilomycin A1.

Coro1a occurs in various types of macrophages. In conclusion, this study demonstrates that Coro1a regulates the autophagosome formation around *M. tuberculosis*-containing phagosomes and assists the survival of infected mycobacteria in macrophages.

Experimental procedures

Cell and bacterial cultures

Raw264.7 and MH-S macrophage cell lines were obtained from the American Type Culture Collection and maintained at 37°C

under a humidified condition with 5% CO_2 in Dulbecco's modified Eagle's medium (DMEM; Sigma-Aldrich, St. Louis, MO) supplemented with 10% fetal bovine serum (FBS; Invitrogen, Carlsbad, CA), 25 μg ml^{-1} penicillin G and 25 μg ml^{-1} streptomycin. BMDM were differentiated from BALB/c mice bone marrow for 7 days in DMEM supplemented with 20% L929-conditioned medium, 10% FBS and antibiotics. *M. tuberculosis* Erdman was obtained from the Japan Research Institute of Tuberculosis, Tokyo, Japan, and grown to mid-logarithmic phase in 7H9 medium supplemented with 10% Middlebrook ADC (BD Biosciences, San Jose, CA), 0.5% glycerol and 0.05% Tween 80 (*Mycobacterium* complete medium) at 37°C. Mycobacteria transformed with a plasmid encoding DsRed were grown in *Mycobacterium* complete medium containing 25 μg ml^{-1} kanamycin.

RNA interference

siRNA duplexes were synthesized by Sigma-Aldrich according to the following sequences: Coro1a#1, sense 5′-GACUGGA CGAGUAGACAAGTT-3′, antisense 5′-CUUGUCUACUCGUCC AGUCTT-3′ (Jayachandran *et al.*, 2008); Coro1a#2 sense 5′-GCAAGACUGGACGAGUAGATT-3′, antisense 5′-UCUACU CGUCCAGUCUUGCTT-3′; Atg3#1, sense 5′-GGUGUAAACA GAUGGAGUATT-3′, antisense 5′-UACUCCAUCUGUUUACACC TT-3′; Atg3#2, sense 5′-GCAUAUCUUCCGACAGACATT-3′, antisense 5′-UGUCUGUCGGAAGAUAUGCTT-3′; Atg5#1, sense 5′-GCUUUACUCUCUAUCAGGATT-3′, antisense 5′-UC CUGAUAGAGAGUAAAGCTT-3′; Atg5#2, sense 5′-GAGACAA GAAGAUGUUAGUTT-3′, antisense 5′-ACUAACAUCUUCUUG UCUCTT-3′; Beclin1#1, sense 5′-GAAAGAUGCUUUAA AUUAATT-3′, antisense 5′-UUAAUUUAAAGCAUCUUUCTT-3′. Beclin1#2, sense 5′-CUGAGAAUGAAUGUCAGAATT-3′, antisense 5′-UUCUGACAUUCAUUCUCAGTT-3′; Mission siRNA universal negative control (Sigma-Aldrich) was used as scrambled siRNA. Transfection of macrophages with siRNA duplexes was performed using Lipofectamine RNAiMAX (Invitrogen) according to the manufacturer's instructions.

Colony-forming unit (cfu) assay

Macrophages transfected with siRNA were grown in 24-well plates at 1×10^5 cells for 24 h, and subsequently infected with *M. tuberculosis* at an moi of 10 for 4 h. Infected macrophages were washed with DMEM three times to remove non-infected mycobacteria and then incubated with DMEM and 10% FBS. At 4 and 72 h p.i., infected macrophages were lysed with 1% IGEPAL in phosphate-buffed saline (PBS), serially diluted with *Mycobacterium* complete medium, and inoculated onto 7H10 agar medium supplemented with 10% Middlebrook OADC (BD Biosciences) and 0.5% glycerol. Colony-forming unit was determined as the mean of four plates at each time point.

Antibodies

Rabbit anti-Coro1a polyclonal antibody (Sigma-Aldrich), mouse anti-actin monoclonal antibody (Sigma-Aldrich), rat anti-mouse LAMP1 monoclonal antibody (SouthernBiotech, Birmingham, AL), mouse anti-LC3 monoclonal antibody (MBL, Nagoya, Japan), rabbit anti-LC3 polyclonal antibody (Sigma-Aldrich), rabbit anti-Atg3 polyclonal antibody (Sigma-Aldrich), rabbit anti-Atg5 polyclonal antibody (Sigma-Aldrich), rabbit anti-Beclin1 polyclonal antibody (Sigma-Aldrich), rabbit anti-p62 polyclonal antibody (MBL), mouse anti-ubiquitin monoclonal antibody (FK2, MBL), mouse anti-Rab7 monoclonal antibody (Abcam, Cambridge, UK), rabbit anti-phospho-ERK1/2 antibody (CST, Denver, MA), rabbit anti-phospho-p38 antibody (CST), rabbit anti-phospho-JNK antibody (CST) and mouse anti-Bcl-2 monoclonal antibody (BD Biosciences) were used for experiments. Alexa488- and Alexa546-conjugated anti-IgG antibodies (Invitrogen) and horseradish peroxidase-conjugated anti-IgG antibodies (Dako, Glostrup, Denmark) were also commercially purchased.

Immunoblot analysis and fluorescence microscopy

Transfected macrophages were extracted by the cell lysis buffer containing 25 mM Tris-HCl pH 7.6, 150 mM NaCl, 1% NP-40, 1% sodium deoxycholate, 0.1% SDS, 100 μM vanadate and protease inhibitor cocktail (Roche, Mannheim, Germany). For immunoblot analysis, cell lysates were separated by SDS-polyacrylamide gel electrophoresis (SDS-PAGE) and then subjected to immunoblot analysis using anti-Coro1a antibody (1:500 v/v), anti-actin antibody (1:1000 v/v), rabbit anti-LC3 polyclonal antibody (1:250 v/v), anti-Atg3 antibody (1:200 v/v), anti-Atg5 antibody (1:300 v/v), anti-Beclin1 antibody (1:100 v/v), anti-Rab7 antibody (1:300 v/v), phospho-ERK1/2 antibody (1:100 v/v), phospho-p38 antibody (1:100 v/v), phospho-JNK antibody (1:100 v/v) or anti-Bcl-2 antibody (1:100 v/v). Band intensity from three independent experiments was quantified using ImageJ (http://rsbweb.nih.gov/ij/). To label lysosomal vesicles with fluorescent dextran, macrophages were incubated with Alexa488-dextran (Invitrogen) at 100 μg ml^{-1} for 12 h. Labelled cells were washed and chased in fluorescent dextran free DMEM with 10% FBS for 6 h.

Immunofluorescence microscopic analysis was performed as previously described (Seto *et al.*, 2009). Macrophages were stained with anti-LAMP1 antibody (1:10 v/v), mouse anti-LC3 monoclonal antibody (1:10 v/v), anti-p62 antibody (1:10 v/v) or anti-ubiquitin antibody (1:10 v/v). Fluorescence microscopy was performed using a LS-1 laser scanning confocal microscope (LSCM; Yokogawa, Tokyo, Japan).

Transfection of macrophages with plasmid

pEGFP-LC3 plasmid was generously provided by Dr Tamotsu Yoshimori (Osaka University, Suita, Japan) and used to transfect Raw264.7 macrophages using an MP-100 electroporator (Digital Bio Technology, Seoul, Korea), according to the manufacturer's instructions. Transfected macrophages were incubated in DMEM with 10% FBS for 24 h prior to the experiments.

Infection of mycobacteria

Transfected macrophages with siRNA grown for 48 h were scraped and grown on round coverslips in 12-well plates for further 12 h. Mycobacteria were washed three times with PBS containing 0.05% Tween 80 and then suspended in DMEM with 10% FBS at a multiplicity of infection (moi) of 30. Aliquots of

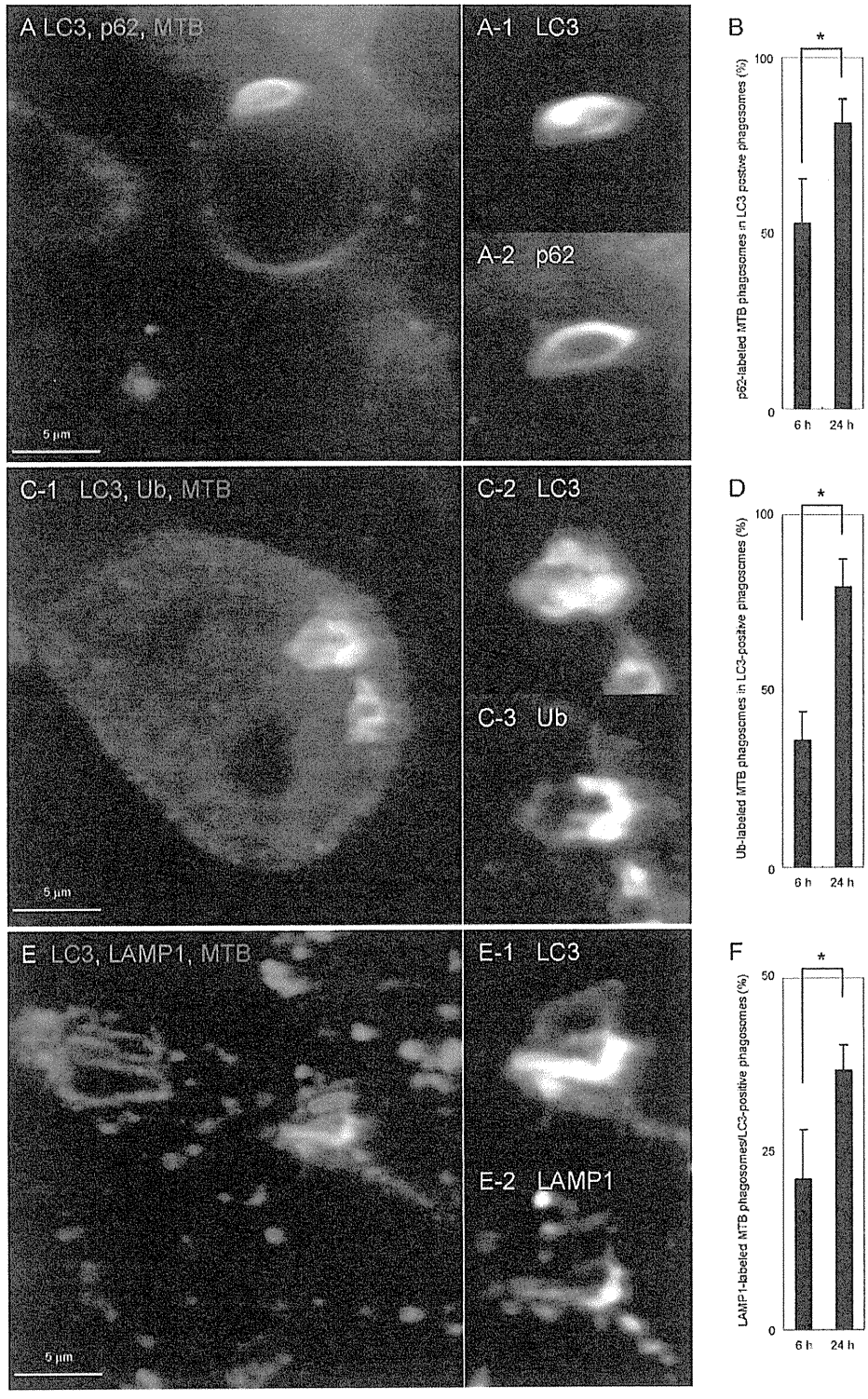
A LC3, p62, MTB
A-1 LC3
A-2 p62
5 μm
B
p62-labeled MTB phagosomes in LC3 positive phagosomes (%)
100
50
0
6 h
24 h
*
C-1 LC3, Ub, MTB
C-2 LC3
C-3 Ub
5 μm
D
Ub-labeled MTB phagosomes in LC3-positive phagosomes (%)
100
50
0
6 h
24 h
*
E LC3, LAMP1, MTB
E-1 LC3
E-2 LAMP1
5 μm
F
LAMP1-labeled MTB phagosomes/LC3-positive phagosomes (%)
50
25
0
6 h
24 h
*

Fig. 8. Recruitment of p62, ubiquitin or LAMP1 to LC3-positive *M. tuberculosis*-containing phagosomes in Coro1a KD macrophages.
A, C and E. Raw264.7 macrophages stably expressing EGFP-LC3 were transfected with Coro1a-specific siRNA for 48 h. Transfected macrophages were infected with Alexa405-labelled *M. tuberculosis* for 24 h and then stained with anti-p62 (A), anti-ubiquitin (C) or anti-LAMP1 (E) antibodies. Enlarged images of A-1, C-1 and E-1 are represented in A-2 and A-3, B-2 and B-3, and C-2 and C-3 respectively.
B, D and F. The proportion of mycobacterial phagosomes labelled with p62 (B), ubiquitin (C) or LAMP1 (F) to the total LC3-positive ones in Coro1a KD macrophages. Macrophages stably expressing EGFP-LC3 were transfected with Coro1a siRNA, and infected with Alexa405-labelled *M. tuberculosis* for 6 or 24 h. Infected macrophages were stained with anti-p62 (B), anti-ubiquitin (D) or anti-LAMP1 (F) antibodies. The numbers of LC3-positive mycobacterial phagosomes labelled with these markers were counted. Data represent the mean and SD of three independent experiments in which more than 100 phagosomes were counted for each condition. $^*P < 0.05$ (unpaired Student's *t*-test). Sc, scrambled; Coro, Coro1a; MTB, *M. tuberculosis*; Ub, ubiquitin.

bacterial suspension were added to 3×10^5 cells of Raw264.7 macrophages on coverslips in 12-well plates, followed by centrifugation at 150 *g* for 5 min and incubation for 10 min at 37°C. Infected cells on coverslips were washed three times with DMEM to remove non-phagocytosed bacteria and then incubated with DMEM containing 10% FBS. At the indicated time points, infected cells were fixed with 3% paraformaldehyde in PBS. For immunoblot analysis to detect the phosphorylation of MAPK, macrophages transfected with siRNA grown for 48 h in six-well plates were infected with *M. tuberculosis* at an moi of 30, and then centrifuged for 5 min and incubated for 10 min at 37°C. Infected cells were washed with DMEM to remove non-infected bacteria and then incubated with DMEM containing 10% of FBS. At the indicated time points, infected cells were washed three times with PBS and extracted with the cell lysis buffer.

Thin-section electron microscopy

Raw264.7 macrophages transfected with siRNA in six-well plates were infected with *M. tuberculosis* at an moi of 30 for 2 h, washed three times with DMEM to remove non-infected bacteria, and further incubated in DMEM with 10% FBS for 4 h. Infected macrophages were fixed with 1% glutaraldehyde in 0.1 M cacodylic acid buffer. Fixed macrophages were incubated with 0.1% (w/v) osmium tetroxide. Cells were dehydrated with a series of ethanol washes and treated with propylene oxide. Samples were embedded in Qetol812 resin (OKEN, Tokyo, Japan) according to the manufacturer's protocol. Thin sections were cut with diamond knives and mounted on copper grids. Samples on grids were counter stained with 2% (w/v) uranyl acetate, and then observed with a JEM-1220 electron microscope (JEOL, Tokyo, Japan).

Isolation of M. tuberculosis*-containing phagosomes*

Six 15 cm dishes of Raw264.7 macrophages were used for each condition. Transfection of macrophages with Coro1a or scrambled siRNA was performed using an MP-100 electroporator according to the manufacturer's instructions. Briefly, 6×10^6 Raw264.7 macrophages were transfected with 1.2 nmol of siRNA per plate. Transfected macrophages were incubated in DMEM with 10% FBS for 48 h prior to the experiments. Raw264.7 macrophages transfected with siRNA were infected with mycobacteria at an moi of 30 for 2 h, washed with DMEM three times to remove non-infected mycobacteria, and further incubated in DMEM with 10% FBS for 4 h. Preparation of isolated mycobacterial phagosomes was performed as described previously (Beatty *et al.*, 2002; Seto *et al.*, 2011).

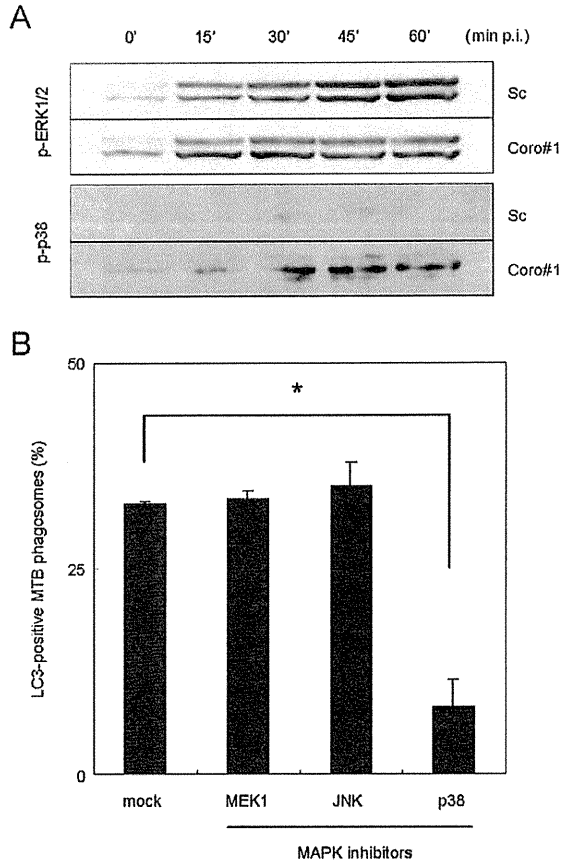

Fig. 9. Differential contribution of MAPK to autophagosome formation around *M. tuberculosis*-containing phagosomes in Coro1a KD macrophages.
A. Phosphorylation of p38 MAPK in Coro1a KD macrophages infected with *M. tuberculosis*. Macrophages transfected with Coro1a-specific or scrambled siRNA were infected with *M. tuberculosis* for the indicated time periods. Whole-cell lysates were subjected to SDS-PAGE, followed by immunoblot analysis using the indicated antibodies.
B. The proportion of LC3-positive *M. tuberculosis*-containing phagosomes in Coro1a KD macrophages treated with MAPK inhibitors. Coro1a KD macrophages expressing EGFP-LC3 were infected with *M. tuberculosis* in the presence of MAPK inhibitors (20 μM) for 6 h. PD98059, SP600125 and SB203580 were used as inhibitors for MEK1, JNK and p38 respectively. Data represent the mean and SD of three independent experiments in which more than 200 phagosomes were counted for each condition. $^*P < 0.05$ (unpaired Student's *t*-test). Sc, scrambled; Coro, Coro1a; Mock, solvent control for MAPK inhibitors (0.1% DMSO).

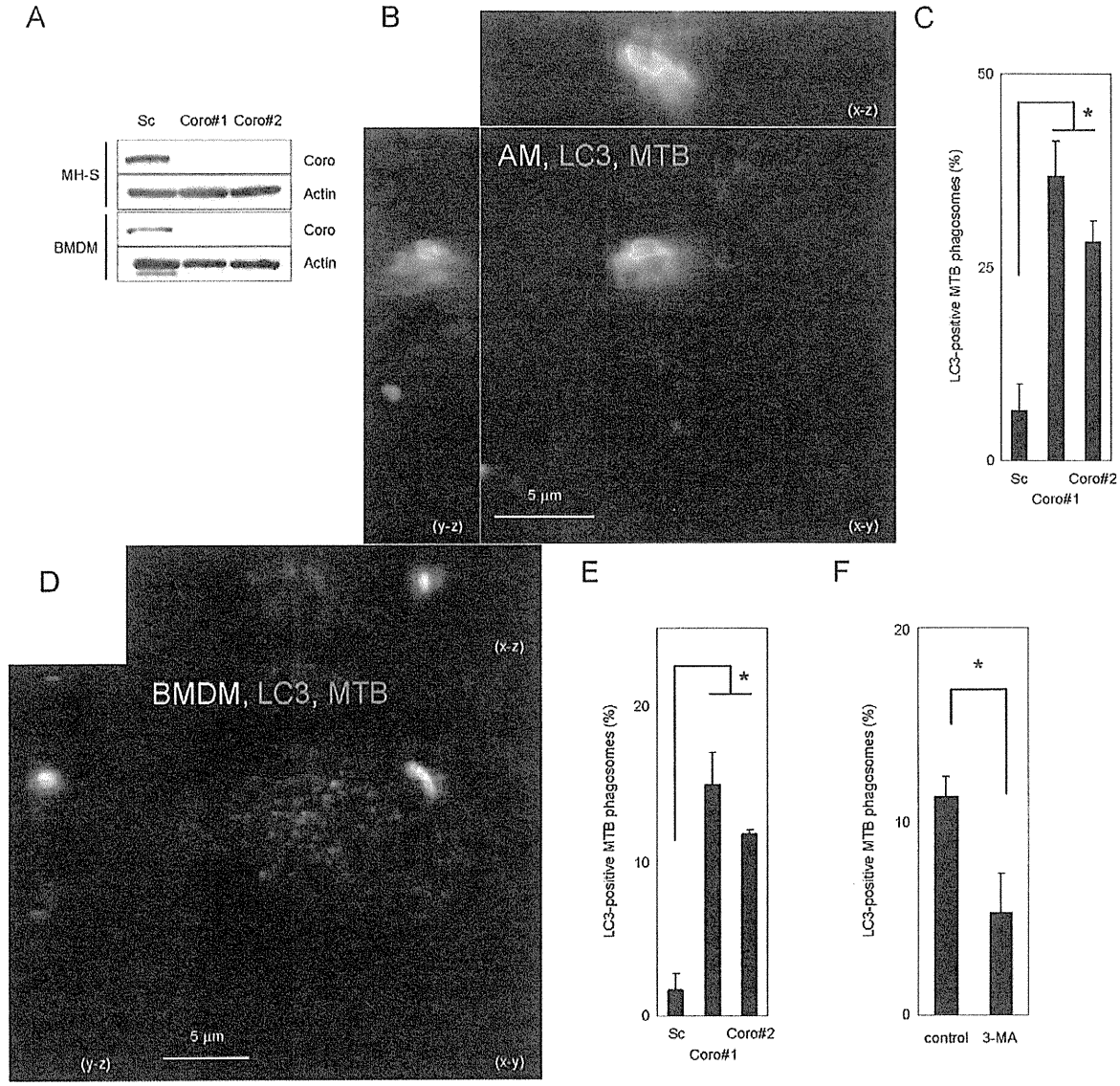

Fig. 10. LC3 recruitment to *M. tuberculosis*-containing phagosomes in the MH-S alveolar macrophage cell line and bone marrow-derived macrophage induced by Coro1a depletion.

A. Immunoblot analysis of MH-S alveolar macrophages (AM) or bone marrow-derived macrophage (BMDM) transfected with Coro1a siRNA. Whole-cell lysates of macrophages transfected with Coro1a or scrambled siRNA were subjected to SDS-PAGE, followed by immunoblot analysis using the indicated antibodies.

B and D. Analysis of LC3 recruitment to *M. tuberculosis*-containing phagosomes in Coro1a KD AM or BMDM. AM (B) or BMDM (D) transfected with Coro1a siRNA were infected with DsRed-expressing *M. tuberculosis* for 6 h. Infected macrophages were fixed and stained with anti-LC3 antibody. Infected macrophages were then observed using LSCM. Projections of focal planes with y–z and x–z side views are represented.

C and E. The proportion of mycobacterial phagosomes labelled with anti-LC3 antibody in AM or BMDM. AM (C) or BMDM (E) were transfected with Coro1a or scrambled siRNA. Transfected macrophages were infected with DsRed-expressing *M. tuberculosis* for 6 h, and then stained with anti-LC3 antibody. LC3-positive phagosomes were counted.

F. 3-MA inhibits the recruitment of LC3 to mycobacterial phagosomes in Coro1a KD BMDM. BMDM were transfected with Coro1a KD siRNA and then treated with or without 3-MA at 10 mM. Macrophages were infected with DsRed-expressing *M. tuberculosis* for 6 h, and then stained with anti-LC3 antibody. The LC3-positive mycobacterial phagosomes were counted. Data represent the mean and SD of three independent experiments in which more than 200 phagosomes were counted for each condition. $^*P < 0.05$ (unpaired Student's *t*-test). Sc, scrambled; Coro, Coro1a; MTB, *M. tuberculosis*; AM, alveolar macrophage cell line MH-S; BMDM, bone marrow-derived macrophage.

Statistics

Paired or unpaired two-sided Student's *t*-tests was used to assess the statistical significance of differences between the two groups. Three or four independent experiments were conducted to assess mycobacterial growth in macrophages, and the number of viable bacteria was determined from the means of four plates. Three independent experiments were conducted to assess the proportions of fluorescence-positive phagosomes.

Acknowledgements

We thank Drs Toshi Nagata and Masato Uchijima (Hamamatsu University School of Medicine, Hamamatsu, Japan) for their helpful discussions. We also thank Ms Keiko Sugaya and Ms Yumiko Suzuki (Hamamatsu University School of Medicine) for their excellent assistance. This work was supported in part by Grants-in-Aid for Young Scientists (B), Scientific Research (B) and Scientific Research (C) from the Japan Society for the Promotion of Science; Scientific Research on Priority Areas from the Ministry of Education, Culture, Sports, Science and Technology of Japan; the Health and Labour Science Research Grants for Research into Emerging and Reemerging Infectious Diseases from the Ministry of Health, Labour and Welfare of Japan; and the United States-Japan Cooperative Medical Science Committee.

References

Alonso, S., Pethe, K., Russell, D.G., and Purdy, G.E. (2007) Lysosomal killing of Mycobacterium mediated by ubiquitin-derived peptides is enhanced by autophagy. *Proc Natl Acad Sci USA* **104:** 6031–6036.

Anand, P.K., and Kaul, D. (2003) Vitamin D3-dependent pathway regulates TACO gene transcription. *Biochem Biophys Res Commun* **310:** 876–877.

Armstrong, J.A., and Hart, P.D. (1971) Response of cultured macrophages to *Mycobacterium tuberculosis*, with observations on fusion of lysosomes with phagosomes. *J Exp Med* **134:** 713–740.

Beatty, W.L., Rhoades, E.R., Hsu, D.K., Liu, F.T., and Russell, D.G. (2002) Association of a macrophage galactoside-binding protein with *Mycobacterium*-containing phagosomes. *Cell Microbiol* **4:** 167–176.

Clemens, D.L., and Horwitz, M.A. (1995) Characterization of the *Mycobacterium tuberculosis* phagosome and evidence that phagosomal maturation is inhibited. *J Exp Med* **181:** 257–270.

Deretic, V., and Levine, B. (2009) Autophagy, immunity, and microbial adaptations. *Cell Host Microbe* **5:** 527–549.

Deretic, V., Vergne, I., Chua, J., Master, S., Singh, S.B., Fazio, J.A., and Kyei, G. (2004) Endosomal membrane traffic: convergence point targeted by *Mycobacterium tuberculosis* and HIV. *Cell Microbiol* **6:** 999–1009.

Deretic, V., Singh, S., Master, S., Harris, J., Roberts, E., Kyei, G., *et al.* (2006) *Mycobacterium tuberculosis* inhibition of phagolysosome biogenesis and autophagy as a host defence mechanism. *Cell Microbiol* **8:** 719–727.

Deretic, V., Delgado, M., Vergne, I., Master, S., De Haro, S., Ponpuak, M., and Singh, S. (2009) Autophagy in immunity against mycobacterium tuberculosis: a model system to dissect immunological roles of autophagy. *Curr Top Microbiol Immunol* **335:** 169–188.

Dupont, N., Lacas-Gervais, S., Bertout, J., Paz, I., Freche, B., Van Nhieu, G.T., *et al.* (2009) Shigella phagocytic vacuolar membrane remnants participate in the cellular response to pathogen invasion and are regulated by autophagy. *Cell Host Microbe* **6:** 137–149.

Dwivedi, M., Song, H.O., and Ahnn, J. (2009) Autophagy genes mediate the effect of calcineurin on life span in *C. elegans*. *Autophagy* **5:** 604–607.

Esclatine, A., Chaumorcel, M., and Codogno, P. (2009) Macroautophagy signaling and regulation. In *Autophagy in Infection and Immunity*. Levine, B., Yoshimori, T., and Deretic, V. (eds). Berlin: Springer, pp. 33–70.

Eskelinen, E.L. (2005) Maturation of autophagic vacuoles in mammalian cells. *Autophagy* **1:** 1–10.

Ferrari, G., Langen, H., Naito, M., and Pieters, J. (1999) A coat protein on phagosomes involved in the intracellular survival of mycobacteria. *Cell* **97:** 435–447.

Galkin, V.E., Orlova, A., Brieher, W., Kueh, H.Y., Mitchison, T.J., and Egelman, E.H. (2008) Coronin-1A stabilizes F-actin by bridging adjacent actin protomers and stapling opposite strands of the actin filament. *J Mol Biol* **376:** 607–613.

Gao, L.Y., Guo, S., McLaughlin, B., Morisaki, H., Engel, J.N., and Brown, E.J. (2004) A mycobacterial virulence gene cluster extending RD1 is required for cytolysis, bacterial spreading and ESAT-6 secretion. *Mol Microbiol* **53:** 1677–1693.

Gutierrez, M.G., Master, S.S., Singh, S.B., Taylor, G.A., Colombo, M.I., and Deretic, V. (2004) Autophagy is a defense mechanism inhibiting BCG and *Mycobacterium tuberculosis* survival in infected macrophages. *Cell* **119:** 753–766.

Hingley-Wilson, S.M., Sambandamurthy, V.K., and Jacobs, W.R., Jr (2003) Survival perspectives from the world's most successful pathogen, *Mycobacterium tuberculosis*. *Nat Immunol* **4:** 949–955.

de Hostos, E.L. (1999) The coronin family of actin-associated proteins. *Trends Cell Biol* **9:** 345–350.

Jagannath, C., Lindsey, D.R., Dhandayuthapani, S., Xu, Y., Hunter, R.L., Jr, and Eissa, N.T. (2009) Autophagy enhances the efficacy of BCG vaccine by increasing peptide presentation in mouse dendritic cells. *Nat Med* **15:** 267–276.

Jayachandran, R., Sundaramurthy, V., Combaluzier, B., Mueller, P., Korf, H., Huygen, K., *et al.* (2007) Survival of mycobacteria in macrophages is mediated by coronin 1-dependent activation of calcineurin. *Cell* **130:** 37–50.

Jayachandran, R., Gatfield, J., Massner, J., Albrecht, I., Zanolari, B., and Pieters, J. (2008) RNA interference in J774 macrophages reveals a role for coronin 1 in mycobacterial trafficking but not in actin-dependent processes. *Mol Biol Cell* **19:** 1241–1251.

Jo, E.K. (2010) Innate immunity to mycobacteria: vitamin D and autophagy. *Cell Microbiol* **12:** 1026–1035.

Kabeya, Y., Mizushima, N., Ueno, T., Yamamoto, A., Kirisako, T., Noda, T., *et al.* (2000) LC3, a mammalian homologue of yeast Apg8p, is localized in autophagosome membranes after processing. *EMBO J* **19:** 5720–5728.

Kumar, D., Nath, L., Kamal, M.A., Varshney, A., Jain, A., Singh, S., and Rao, K.V. (2010) Genome-wide analysis of the host intracellular network that regulates survival of *Mycobacterium tuberculosis*. *Cell* **140:** 731–743.

Lerena, M.C., and Colombo, M.I. (2011) *Mycobacterium marinum* induces a marked LC3 recruitment to its containing phagosome that depends on a functional ESX-1 secretion system. *Cell Microbiol* **13:** 814–835.

Lerena, M.C., Vazquez, C.L., and Colombo, M.I. (2010) Bacterial pathogens and the autophagic response. *Cell Microbiol* **12:** 10–18.

Levine, B. (2005) Eating oneself and uninvited guests: autophagy-related pathways in cellular defense. *Cell* **120:** 159–162.

Mbawuike, I.N., and Herscowitz, H.B. (1989) MH-S, a murine alveolar macrophage cell line: morphological, cytochemical, and functional characteristics. *J Leukoc Biol* **46:** 119–127.

Mizushima, N., and Levine, B. (2010) Autophagy in mammalian development and differentiation. *Nat Cell Biol* **12:** 823–830.

Mueller, P., Liu, X., and Pieters, J. (2011) Migration and homeostasis of naive T cells depends on coronin 1-mediated prosurvival signals and not on coronin 1-dependent filamentous actin modulation. *J Immunol* **186:** 4039–4050.

Pattingre, S., Tassa, A., Qu, X., Garuti, R., Liang, X.H., Mizushima, N., *et al.* (2005) Bcl-2 antiapoptotic proteins inhibit Beclin 1-dependent autophagy. *Cell* **122:** 927–939.

Perrin, A.J., Jiang, X., Birmingham, C.L., So, N.S., and Brumell, J.H. (2004) Recognition of bacteria in the cytosol of mammalian cells by the ubiquitin system. *Curr Biol* **14:** 806–811.

Pethe, K., Swenson, D.L., Alonso, S., Anderson, J., Wang, C., and Russell, D.G. (2004) Isolation of *Mycobacterium tuberculosis* mutants defective in the arrest of phagosome maturation. *Proc Natl Acad Sci USA* **101:** 13642–13647.

Pieters, J. (2008) Coronin 1 in innate immunity. *Subcell Biochem* **48:** 116–123.

Ponpuak, M., Davis, A.S., Roberts, E.A., Delgado, M.A., Dinkins, C., Zhao, Z., *et al.* (2011) Delivery of cytosolic components by autophagic adaptor protein p62 endows autophagosomes with unique antimicrobial properties. *Immunity* **32:** 329–341.

Russell, D.G. (2001) *Mycobacterium tuberculosis*: here today, and here tomorrow. *Nat Rev Mol Cell Biol* **2:** 569–577.

Russell, D.G. (2007) Who puts the tubercle in tuberculosis? *Nat Rev Microbiol* **5:** 39–47.

Seglen, P.O., and Gordon, P.B. (1982) 3-Methyladenine: specific inhibitor of autophagic/lysosomal protein degradation in isolated rat hepatocytes. *Proc Natl Acad Sci USA* **79:** 1889–1892.

Seto, S., Matsumoto, S., Ohta, I., Tsujimura, K., and Koide, Y. (2009) Dissection of Rab7 localization on *Mycobacterium tuberculosis* phagosome. *Biochem Biophys Res Commun* **387:** 272–277.

Seto, S., Matsumoto, S., Tsujimura, K., and Koide, Y. (2010) Differential recruitment of CD63 and Rab7-interacting-lysosomal-protein to phagosomes containing *Mycobacterium tuberculosis* in macrophages. *Microbiol Immunol* **54:** 170–174.

Seto, S., Tsujimura, K., and Koide, Y. (2011) Rab GTPases regulating phagosome maturation are differentially recruited to mycobacterial phagosomes. *Traffic* **12:** 407–420.

Shin, D.M., Jeon, B.Y., Lee, H.M., Jin, H.S., Yuk, J.M., Song, C.H., *et al.* (2010) *Mycobacterium tuberculosis* eis regulates autophagy, inflammation, and cell death through redox-dependent signaling. *PLoS Pathog* **6:** e1001230.

Singh, S.B., Davis, A.S., Taylor, G.A., and Deretic, V. (2006) Human IRGM induces autophagy to eliminate intracellular mycobacteria. *Science* **313:** 1438–1441.

Sirakova, T.D., Dubey, V.S., Kim, H.J., Cynamon, M.H., and Kolattukudy, P.E. (2003) The largest open reading frame (pks12) in the *Mycobacterium tuberculosis* genome is involved in pathogenesis and dimycocerosyl phthiocerol synthesis. *Infect Immun* **71:** 3794–3801.

Smith, J., Manoranjan, J., Pan, M., Bohsali, A., Xu, J., Liu, J., *et al.* (2008) Evidence for pore formation in host cell membranes by ESX-1-secreted ESAT-6 and its role in *Mycobacterium marinum* escape from the vacuole. *Infect Immun* **76:** 5478–5487.

Stamm, L.M., Morisaki, J.H., Gao, L.Y., Jeng, R.L., McDonald, K.L., Roth, R., *et al.* (2003) *Mycobacterium marinum* escapes from phagosomes and is propelled by actin-based motility. *J Exp Med* **198:** 1361–1368.

Sugaya, K., Seto, S., Tsujimura, K., and Koide, Y. (2011) Mobility of late endosomal and lysosomal markers on phagosomes analyzed by fluorescence recovery after photobleaching. *Biochem Biophys Res Commun* **410:** 371–375.

Vergne, I., Chua, J., and Deretic, V. (2003) *Mycobacterium tuberculosis* phagosome maturation arrest: selective targeting of PI3P-dependent membrane trafficking. *Traffic* **4:** 600–606.

Vergne, I., Chua, J., Singh, S.B., and Deretic, V. (2004) Cell biology of *Mycobacterium tuberculosis* phagosome. *Annu Rev Cell Dev Biol* **20:** 367–394.

van der Wel, N., Hava, D., Houben, D., Fluitsma, D., van Zon, M., Pierson, J., *et al.* (2007) *M. tuberculosis* and *M. leprae* translocate from the phagolysosome to the cytosol in myeloid cells. *Cell* **129:** 1287–1298.

World Health Organization (2010) *WHO Report 2010 Global Tuberculosis Control.* Geneva: WHO [WWW document]. http://www.who.int/tb/publications/global_report/2010/en/index.html.

Xu, Y., Jagannath, C., Liu, X.D., Sharafkhaneh, A., Kolodziejska, K.E., and Eissa, N.T. (2007) Toll-like receptor 4 is a sensor for autophagy associated with innate immunity. *Immunity* **27:** 135–144.

Yan, M., Collins, R.F., Grinstein, S., and Trimble, W.S. (2005) Coronin-1 function is required for phagosome formation. *Mol Biol Cell* **16:** 3077–3087.

Yuk, J.M., Shin, D.M., Lee, H.M., Yang, C.S., Jin, H.S., Kim, K.K., *et al.* (2009) Vitamin D3 induces autophagy in human monocytes/macrophages via cathelicidin. *Cell Host Microbe* **6:** 231–243.

Zheng, Y.T., Shahnazari, S., Brech, A., Lamark, T., Johansen, T., and Brumell, J.H. (2009) The adaptor protein p62/

SQSTM1 targets invading bacteria to the autophagy pathway. *J Immunol* **183:** 5909–5916.

Supporting information

Additional Supporting Information may be found in the online version of this article:

Fig. S1. Immunoblot analysis of LC3 in macrophages infected with *M. tuberculosis* at deferent moi.
A. Raw264.7 macrophages were transfected with Coro1a-specific or scrambled siRNA. Transfected macrophages were infected with *M. tuberculosis* at different moi for 6 h. Whole-cell lysates were subjected to SDS-PAGE, followed by immunoblot analysis using the indicated antibodies.
B. The band intensity for LC3-II per Rab7 at each condition to that in the macrophage without infection is shown. The data represent the mean and SD of three independent experiments. N.S., not significant (paired Student's *t*-test); MTB, *M. tuberculosis*; Sc, scrambled; Coro, Coro1a.
Fig. S2. Phagocytosis of latex beads and infection by *M. tuberculosis* in Coro1a KD macrophage. Raw264.7 macrophages were transfected with Coro1a-specific or scrambled siRNA for 48 h. Transfected macrophages were phagocytosed by FITC-labelled latex beads or DsRed-expressing *M. tuberculosis*. The rate of phagocytosed or infected macrophages were analysed by flow cytometry or fluorescent microscopy respectively. The data represent the mean and SD of three independent experiments. N.S., not significant (paired Student's *t*-test); MTB, *M. tuberculosis*; Sc, scrambled; Coro, Coro1a.
Fig. S3. LC3 recruitment to mycobacterial phagosomes in macrophages treated with calcineurin inhibitors. Macrophages stably expressing EGFP-LC3 were treated with FK506 (0.5 μM) or cyclosporine A (0.1 μM) for 1 h, and then infected with DsRed-expressing *M. tuberculosis* for 6 h. Cells were fixed and observed with LSCM. The number of LC3-positive *M. tuberculosis* phagosomes was counted. Data represent the mean and SD of three independent experiments in which more than 200 phagosomes were counted for each condition. N.S., not significant (unpaired Student's *t*-test); FK, FK506; Cyc, cyclosporine A; MTB, *M. tuberculosis*.
Fig. S4. Bcl-2 expression in Coro1a KD macrophages. Raw264.7 macrophages were transfected with Coro1a-specific siRNA for 48 h. Whole-cell lysates were subjected to SDS-PAGE, followed by immunoblot analysis using anti-Bcl-2 or anti-Coro1a antibodies. Bec1, Beclin1; Sc, scrambled; Coro, Coro1a.

Please note: Wiley-Blackwell are not responsible for the content or functionality of any supporting materials supplied by the authors. Any queries (other than missing material) should be directed to the corresponding author for the article.

Infection, Genetics and Evolution 12 (2012) 1392–1396

Contents lists available at SciVerse ScienceDirect

Infection, Genetics and Evolution

journal homepage: www.elsevier.com/locate/meegid

Scanning of genetic diversity of evolutionarily sequential *Mycobacterium tuberculosis* Beijing family strains based on genome wide analysis

Takayuki Wada [a,*], Tomotada Iwamoto [b], Atsushi Hase [a], Shinji Maeda [c]

[a] *Department of Microbiology, Osaka City Institute of Public Health and Environmental Sciences, 8-34 Tojo-cho, Tennoji-ku, Osaka 543-0026, Japan*
[b] *Department of Microbiology, Kobe Institute of Health, 4-6 Minatojima-Nakamachi, Chuo-ku, Kobe 650-0046, Japan*
[c] *Department of Mycobacterium Reference and Research, The Research Institute of Tuberculosis, Japan Anti-Tuberculosis Association, 3-1-24 Matsuyama, Kiyose, Tokyo 204-8533, Japan*

ARTICLE INFO

Article history:
Received 1 March 2012
Received in revised form 28 April 2012
Accepted 30 April 2012
Available online 9 May 2012

Keywords:
Mycobacterium tuberculosis
Beijing family
Genetic diversity
Genomics
Molecular epidemiology
Genotyping

ABSTRACT

The Beijing family is an endemic lineage of *Mycobacterium tuberculosis* in eastern Asia. In Japan, five evolutionarily sequential sublineages composing the lineage have predominated. Comparative genomic sequencing based on a microarray technique was conducted for five representative strains of those respective sublineages. Results revealed approximately 200 point mutations specific to each strain. Subsequently, to investigate the genetic diversity of each sublineage, we analysed the phylogenetic divergence of 103 domestic strains belonging to them using genetic markers derived from the mutation information. Results show that the five sublineages have comprised smaller lineages which had diverged at various points. The smaller sub-sublineages have emerged with respective bottlenecks, which are reflected in the excessive monophyletic evolution of the species. Our data provide necessary information to grasp a comprehensive picture of genetic diversity of the lineage constructed in its evolution.

1. Introduction

A worldwide investigation of clinical strains of *Mycobacterium tuberculosis*, an etiological agent of human tuberculosis, has revealed that the species is classifiable mainly into several monophyletic lineages (Gagneux and Small, 2007). These lineages, which are distributed throughout the world, have predominated over others in some areas. They putatively evolved in their endemic areas and have increased their adaptability against natural selection via the immunity of geographically or ethnically distinct human hosts (Gagneux et al., 2006). It is therefore important to ascertain their genetic specificity and diversity, which is expected to reveal their evolutionary strategy as a virulent species against humans.

Lineage 2, Beijing family, is an endemic lineage of *M. tuberculosis* throughout eastern Asia (van Soolingen et al., 1995). Strains belonging to the lineage have been isolated from TB patients in the area with high frequency. Reportedly, Beijing family is phylogenetically divisible into two subfamilies: modern (typical) and ancient (atypical) subfamilies (Mokrousov et al., 2002, 2005). The modern subfamily has been isolated frequently not only in eastern Asia, but also in other distant areas such as western Russia, South Africa, and Thailand (Faksri et al., 2011; Glynn et al., 2002; Hanekom et al., 2007; Mokrousov et al., 2002). These reports encourage the hypothesis that this subfamily might not only adapt to eastern Asian human hosts; it also boosts their substantial virulence during their evolution. However, the ancient subfamily has been regarded as a minor component of the lineage. Most Beijing strains isolated from TB patients throughout the world have been assigned to the modern subfamily. Therefore, the lineage has been regarded as highly clonal (low diversity) and emerging.

An exception to such a global tendency is apparent in Japan (Wada et al., 2009b). There, at the east end of Eurasian continent, Beijing family has strongly predominated (about 80% of all isolates), as it has also in surrounding countries. In contrast to the global tendency, refined population genetic structure analyses have revealed that the ancient subfamily has been mainly endemic in Japan. The Beijing family in Japan has mainly comprised five sublineages, which suggests broader genetic diversity than in other areas (Iwamoto et al., 2009; Wada and Iwamoto, 2009; Wada et al., 2009b). The modern (typical) subfamily has been regarded as only one component of them. Reasons that such a unique population structure of the lineage is observed remain elusive. Population genetic structures in Japan were reportedly similar regardless of origin areas in the country (Wada et al., 2009a; Maeda et al., 2010; Millet et al., 2012; Yokoyama et al., 2012). The extent of their genetic diversity and characterisation of genomic features also remain unclear. It is expected to be a suitable population model for investigating the microevolutionary process of the lineage.

* Corresponding author. Tel.: +81 6 6771 3148; fax: +81 6 6772 0676.
E-mail address: taka-wada@city.osaka.lg.jp (T. Wada).

1567-1348/$ - see front matter © 2012 Elsevier B.V. All rights reserved.
http://dx.doi.org/10.1016/j.meegid.2012.04.029

For examination in this study, we selected referential strains from five phylogenetically robust sublineages to refine their genetic features based on comparative genomics. Subsequently, information of representative mutations found in the previous analysis was used to analyse clinical strains of each sublineage reversely, thereby yielding an estimate of their genetic diversity.

2. Materials and methods

2.1. Genotypic definition

Sublineages of Beijing lineage were determined phylogenetically according to previous reports, using large-sequence polymorphisms (LSP, RD181, RD150, and RD142), and IS*6110* insertion in the NTF to classify the ancient/modern subfamilies, and using types of sequences (STs) to confirm their sublineages (Filliol et al., 2006; Tsolaki et al., 2005; Wada et al., 2009b). STs were roughly defined by Filliol's 10 SNPs (Filliol et al., 2006), but 909166 (C -> T) was excluded from our definition because of duplication of a gene encompassing the position (*cysA2*) on a genome and its ambiguous homoplasy (Faksri et al., 2011). Alternatively, 1576481 (T -> G) was introduced from a Supplementary table of SNPs by Filliol et al. (2006) to compensate the subdivision by 909166, which discriminates two major STs (STK and ST3) of Beijing strains populations in Japan (Iwamoto et al., 2009; Wada and Iwamoto, 2009; Wada et al., 2009b). Sublineages were defined as presented in Table 1.

2.2. Referential strains for comparative genomics

For comparative genomics, five referential *M. tuberculosis* Beijing family strains belonging to main five sublineages in Japan (G1/2, G3, G4, G5/6, and G7) were selected from our collection of clinical isolates (Table 2). Supply's 15-locus variable number of tandem repeats (VNTR) genotypes (Supply et al., 2006) were also analysed to determine their genotypic profiles.

2.3. Preparation of genomic DNA

Genomic DNAs were prepared according to a previous report (Parish and Stoker, 1998). Briefly, five reference strains and H37Rv were cultured on Ogawa media. The bacilli were delipidated using chloroform:methanol (3:1) and then lysed using egg-white lysozyme. Finally, genomic DNA was purified using phenol/chloroform extraction from lysates. The quality and quantity of purified genomic DNAs were checked using OD_{260} and agarose electrophoresis.

2.4. Mutation mapping and determination of point mutations

Tiling arrays for mutation mapping (comparative genomic sequencing, CGS) were designed to cover the whole genomic sequence of H37Rv (EMBL/GenBank/DDBJ entry AL123456.2) (Cole et al., 1998). The oligonucleotide length was determined as 29 m. The interval length was determined as 7 m. Consequently, approximately 490,000 oligonucleotides were labelled on the arrays. Genomic DNAs from Beijing strains and H37Rv were fragmented and conjugated with Cy3 and Cy5 respectively to hybridize to the arrays. Fluorescent signals with differences were flagged as regions of interest (ROIs), which were analysed further as putative point mutations of each strain. Subsequent analysis was performed using 'resequencing arrays', which were designed to cover eight bases of both strands at each nucleotide of ROIs, as previously reported (Albert et al., 2005; Herring and Palsson, 2007), to determine their exact substitutions.

2.5. Mutation analysis for clinical strains

Intergenic mutations identified in the reference strains were verified using PCR and direct sequencing analyses of amplicons from the genomic DNAs of 103 strains, just as reference strains had been. To analyse the sublineages evenly, strains (genotypes) were selected randomly from every sublineage as follows; 16 of 30 genotypes from G1/2; 24 of 85 genotypes from G3; 24 of 73

Table 1
Definitions of sublineages of Beijing family *M. tuberculosis* in this study.

Sublineages definition in this study	Single-nucleotide polymorphism										IS*6110* in the NTF	Large-sequence polymorphism		
	797736	2825581	1576481	1892017	4137829	1477596	2376135	2532616	1548149	1692069		RD181	RD150	RD142
Reference (H37Rv)	C	T	T	T	C	C	A	G	G	A	–	+	+	+
G1/2	C	T	T	T	C	C	A	G	G	A	–	+	+	+
G3	T	G	T	T	C	C	A	G	G	A	–	–	+	+
G4	T	G	G	T	C	C	A	G	G	A	–	–	+	+
G5/6	T	G	G	C	T	C	A	G	G	A	–	–	+	+
G7	T	G	G	C	T	A	A	G	G	A	+	–	+	+
G8	T	G	G	C	T	A	A	G	G	A	+	–	–	+
G9	T	G	G	C	T	A	G	A	G	A	+	–	+	+

Table 2
Characteristics of the Beijing family strains analysed in this study.

Strain name	Sublineage	Origin	Year of isolation	Supply's 15 VNTR*														
				424	577	580	802	960	1644	1955	2163b	2165	2401	2996	3192	3690	4052	4156
A05N056	G1/2	Kobe	2005	3	4	2	2	3	2	4	5	4	4	7	4	3	9	4
ID381	G3	Kobe	2006	4	4	2	3	3	3	3	3	4	2	6	5	3	7	4
4558	G4	Osaka	2007	4	4	2	3	1	3	3	7	4	4	7	5	3	8	5
4994	G5/6	Osaka	2007	3	4	2	3	3	4	3	7	4	4	7	5	3	2	5
4991/M	G7	Osaka	2007	4	4	2	3	3	3	4	8	4	4	7	5	3	8	3
H37Rv	–	–	–	2	4	3	1	3	2	1	5	3	2	3	3	5	5	3

* Variable number of tandem repeats (Supply et al., 2006).

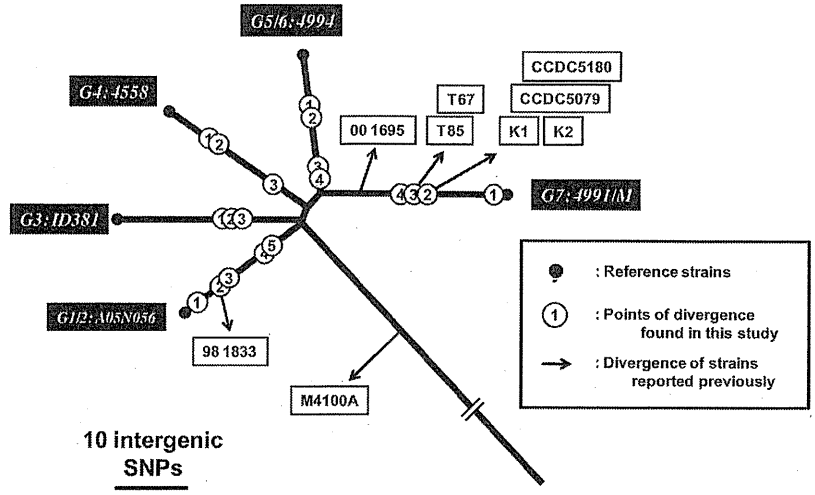

Fig. 1. Schematic phylogenetic tree of *M. tuberculosis* Beijing family based on comparative genomics of strains isolated in Japan. Text boxes show strains analysed using a genome-wide strategy. Black boxes show the five referential strains analysed in this study. Opened boxes (K1, K2, CCDC5079, CCDC5080, M4100A, 98 1833, 00 1695, T67, and T85) show Beijing strains whose genomic data were derived from previous studies (Niemann et al., 2009; Zhang et al., 2011) and a database (TB Database: http://www.tbdb.org/). Numbered circles denote points of phylogenetic divergence found in this study (Table 4).

(several common intergenic mutations; Table 4, Fig. 1). In general, synonymous or intergenic mutations, not related to amino acid changes of proteins, are regarded as poorly related to phenotypes and natural selection of variants. It is expected that such neutral mutations are useful to observe the genetic diversity of a population without a putative bias because of natural selection. Each sublineage has been composed of smaller sublineages. Such a list of SNPs will be constructed by accumulation of genomic data of clinical strains in the future as a genotypic marker to discriminate or define clinical isolates. In this study, the subdivision has remained insufficient in the presence of major sub-components (G3-2, 21 of 24 strains; G4-2, 19 of 24; G5/6-4, 17 of 24; and G7-2, 9 of 15). These results do not signify that the sublineages are homogeneous because their reference strains (ID381 of G3, 4558 of G4, 4994 of G5/6, and 4991/M of G7) might have diverted before the main sub-sublineage emerged. It is necessary to incorporate additional strains for genomic comparison to determine whether the sub-sublineages can be ascertained.

Recently, SNP-based genotypings for *M. tuberculosis* have been reported (Abadia et al., 2010; Luo et al., 2012; Schurch et al., 2011). SNP-based typing can provide a reliable framework of phylogenetic positions of *M. tuberculosis* strains because of its low frequency of homoplasy (Comas et al., 2009). Once an SNP-based genotyping can be established, it will be expected to complement VNTR typing, a standard method to discriminate clinical strains. In contrast to SNPs, VNTR presents the disadvantage of estimating the genetic distance of strains because of its allelic homoplasy (Comas et al., 2009). Actually, correlation between VNTR and phylogenetic positions is not clearly evident, even in our detailed study (Table S4). Refined SNPs information can improve genetic definition of clinical strains of *M. tuberculosis*, which can be helpful for biological research of pathogens. In Japan, aside from the endemic prevalence of the ancient Beijing overall, certain sublineages showed some epidemiological tendencies of TB patients such as drug resistance, age, and the transmission rate (Iwamoto et al., 2008, 2009; Wada et al., 2009a). Genetic information of sublineages retrieved from genome-wide analysis is expected to provide clues to finding genetic causes related to putative phenotypes of clinical strains.

Modern Beijing subfamily is an important target to be studied because of its acute prevalence in worldwide areas. In this study, 108 of 199 point mutations specific to 4991/M were common to the K-backbone (Table 3). This result is consistent with the estimation that K-1 and K-2 belong to the same sublineage as 4991/M (G7) from their mutation repertoires (data not shown). K-1 and K-2 were regarded as belonging to G7-2, as presented in Fig. 1, in our definition. CCDC5079 and CCDC5180, which were isolated in China, were also estimated as belonging to G7-2 from their genome sequences (Zhang et al., 2011). Isolation irrespective of geographical origin supports the hypothesis that the sub-sublineage had spread in broad areas in the past and has become endemic up to now. The population structure of *M. tuberculosis* in Japan, an endemic area of the ancient subfamily, might be inefficient for observation of genetic diversity of the modern subfamily. It is expected that the diversity of modern subfamily will be scrutinised using reasonable populations.

A powerful tool to detect multiple mutations present in one bacterium relative to another, CGS (Herring and Palsson, 2007), has also been used to find specific mutations in targeted strains such as *Helicobacter pylori* and *Streptomyces coelicolor* (Albert et al., 2005; Okamoto et al., 2007). In this study, we were able to detect mutations specific to each strain using CGS to classify our focused sublineages. In fact, NGSs, such as HiSeq (Illumina Inc.), GS-FLX 454 system (Roche Diagnostics Corp.), and SOLID system (Life Technologies Inc.) have been rapidly developed recently. It is expected that continued price reduction of NGS technology and development of bioinformatic tools for use with data will radically accelerate genomic research related to clinical strains of pathogens.

The Beijing family is the most deeply analysed lineage of species from the perspective of its phenotype, phylogeny, and genomics. Fig. 1 shows that genomic information of individual *M. tuberculosis* strains has become mappable into a single tree based on genome-wide comparison, despite the strains' disparate geographical origins. Combining genomic data from various laboratories and incorporating additional strains will enrich such a 'diversity map' of the lineage. That process will lead to comprehension of the overall appearance of the lineage.

Acknowledgements

This work was supported by Grants from the United States–Japan Cooperative Medical Science Program against Tuberculosis and Leprosy, the Ministry of Health, Labour and Welfare, Japan